Synthesis, Radiosynthesis, and Biological Evaluation of Fluorine-18-Labeled 2β-Carbo(fluoroalkoxy)-3β-(3′-((*Z*)-2-haloethenyl)phenyl)nortropanes: Candidate Radioligands for In Vivo Imaging of the Serotonin Transporter with Positron Emission Tomography

Jeffrey S. Stehouwer,[†] Nachwa Jarkas,[†] Fanxing Zeng,[†] Ronald J. Voll,[†] Larry Williams,[†] Vernon M. Camp,[†] Eugene J. Malveaux,[†] John R. Votaw,[†] Leonard Howell,[‡] Michael J. Owens,[§] and Mark M. Goodman*[,†,§]

Department of Radiology, Department of Psychiatry and Behavioral Sciences, and Yerkes National Primate Research Center, Emory University, Atlanta, GA

Received June 27, 2008

The *meta*-vinylhalide fluoroalkyl ester nortropanes **1**−**4** were synthesized as ligands of the serotonin transporter (SERT) for use as positron emission tomography (PET) imaging agents. In vitro competition binding assays demonstrated that **1**−**4** have a high affinity for the SERT (K_i values = 0.3−0.4 nM) and are selective for the SERT over the dopamine and norepinephrine transporters (DAT and NET). MicroPET imaging in anesthetized cynomolgus monkeys with [^{18}F]**1**−[^{18}F]**4** demonstrated that all four tracers behave similarly with peak uptake in the SERT-rich brain regions achieved after 45−55 min, followed by a steady washout. An awake monkey study was performed with [^{18}F]**1**, which demonstrated that the uptake of [^{18}F]**1** was not influenced by anesthesia. Chase studies with the SERT ligand **15** displaced [^{18}F]**1**−[^{18}F]**4**, but chase studies with the DAT ligand **16** did not displace [^{18}F]**1**−[^{18}F]**4** thus indicating that the tracers were binding specifically to the SERT.

Introduction

The human serotonin transporter (SERT)[a] is a 630 amino acid transmembrane protein located in the brain, peripheral organs, and blood platelets.[3−6] Within the central nervous system (CNS), the SERT is localized on the presynaptic terminals of serotonergic neurons and functions to terminate neurotransmission by removing serotonin from the synapse. Serotonergic neurons originate primarily in the median and dorsal raphe nuclei of the brainstem and innervate discrete areas that include the hypothalamus, thalamus, striatum, and cerebral cortex.[4,7−10] Thus, the SERT can serve as a specific marker for serotonergic neuronal anatomy and integrity. Dysregulation of serotonin neurotransmission has been implicated in the pathophysiology of major depression and a reduction in SERT density has been observed postmortem in the tissues of depressed patients and suicide victims.[7,11−14] Therefore, the SERT is the target of the selective serotonin reuptake inhibitor (SSRI) class of antidepressants. The ability to image CNS SERT in vivo using positron emission tomography (PET) [15−17] may provide insight into the pathophysiology of depression and suicide by enabling the SERT density of specific brain regions to be measured, thereby indicating which regions of the brain have SERT density altered by the disease, as well as allow for improved diagnostic techniques and monitoring of antidepressant therapy.[18−22] Furthermore, the availability of SERT PET tracers may aid in the development of new SERT therapeutics by allowing for occupancy measurements of the therapeutic.[23−28]

This need for a SERT PET tracer has led to extensive research into the development of new tracers for this target[17] with the majority of these new compounds belonging to the diarylsulfide[24,29−43] or nortropane[44−46] classes. Many of the initial SERT PET tracers are ^{11}C-labeled compounds and therefore are limited to use in the location where they are prepared due to the short half-life of ^{11}C ($t_{1/2}$ = 20.4 min). Tracers labeled with ^{18}F are desirable because the longer half-life of ^{18}F ($t_{1/2}$ = 109.8 min) allows for longer radiosynthesis times and transport of ^{18}F-labeled tracers to sites away from the production facility which thus enables PET imaging centers without onsite cyclotrons to utilize these tracers. Furthermore, ^{18}F positrons have a lower maximum energy than ^{11}C positrons (0.64 vs 0.97 MeV)[17] and therefore deposit less energy into tissue, and they also have a shorter linear range[47,48] that allows for higher spatial resolution. These properties of ^{18}F are fortuitous because of the valuable role that ^{19}F plays in medicinal chemistry[49−51] and numerous methods have now been developed to incorporate ^{18}F or ^{19}F into molecules.[52−54]

The goal of developing a viable SERT PET tracer is an important, but not easy, task as evidenced by the numerous compounds that have been and continue to be reported. Several criteria need to be met for a candidate molecule to become a useful tracer. The desirable properties for a candidate SERT PET tracer include (exceptions may exist) (1) high binding affinity[55] (K_i = ∼0.1−0.5 nM) for the SERT with high selectivity (>50:1) over the norepinephrine transporter (NET) and dopamine transporter (DAT); (2) moderate lipophilicity (log P = ∼1−3)[56−58] for good initial brain entry and low nonspecific binding; (3) high uptake ratios versus cerebellum[59] (≥1.7) in SERT-rich brain regions, such as thalamus, hypothalamus, and raphe, with uptake ratios ≥1.3 in low density regions such as anterior cingulate to enable delineation of specific SERT binding; (4) specific binding to brain SERT reaching peak equilibrium at ≤60 min, followed by washout for both ^{11}C-

* To whom correspondence should be addressed. Address: Department of Radiology, Emory University, 1364 Clifton Road NE, Atlanta, GA 30322. Phone: (404) 727-9366. Fax: (404) 727-3488. E-mail: mgoodma@emory.edu.

[†] Department of Radiology.

[§] Department of Psychiatry and Behavioral Sciences.

[‡] Yerkes National Primate Research Center.

[a] Abbreviations: PET, positron emission tomography; SUV, standardized uptake value;[1,2] SPECT, single-photon emission computed tomography; TAC, time-activity curve; HRRT, high resolution research tomograph; EOB, end-of-bombardment; CNS, central nervous system; SSRI, selective serotonin reuptake inhibitor; SERT, serotonin transporter; DAT, dopamine transporter; NET, norepinephrine transporter.

10.1021/jm800781a CCC: $40.75
Published on Web 11/24/2008

Scheme 1

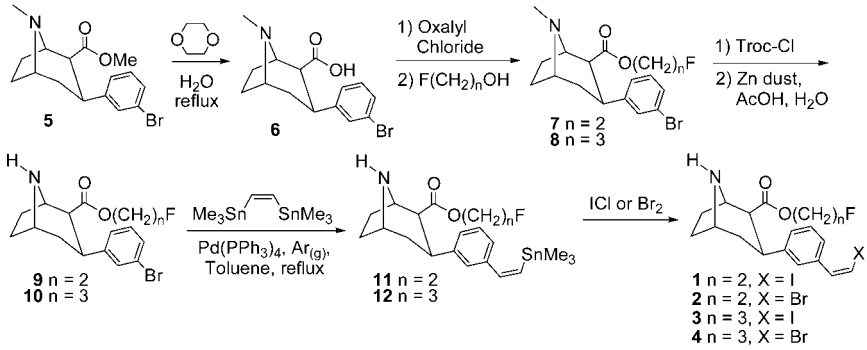

Scheme 2

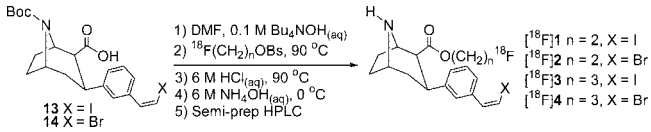

and ^{18}F-tracers to allow quantification of SERT occupancy; (5) lack of radiolabeled metabolites generated in the brain; and (6) lack of lipophilic radiolabeled metabolites in peripheral organs that may enter brain and bind specifically or nonspecifically to SERT-rich regions and cerebellum.

As part of an ongoing research project in our laboratories to develop SERT-selective tropane and nortropane PET and single-photon emission computed tomography (SPECT) imaging agents labeled with ^{11}C or ^{18}F (PET) or ^{123}I (SPECT) for human diagnostic applications we have been exploring the effect of placing a vinyl halide[60−66] or furyl substituent[67] on the 3β-phenyl ring. We report here the synthesis and biological evaluation of 2β-carbo(2-fluoroethoxy)-3β-(3′-((*Z*)-2-iodoethenyl)phenyl)nortropane (**1**, FE*m*ZIENT),[68] 2β-carbo(2-fluoroethoxy)-3β-(3′-((*Z*)-2-bromoethenyl)phenyl)nortropane (**2**, FE*m*ZBrENT),[69] 2β-carbo(3-fluoropropoxy)-3β-(3′-((*Z*)-2-iodoethenyl)phenyl)nortropane (**3**, FP*m*ZIENT),[70] and 2β-carbo(3-fluoropropoxy)-3β-(3′-((*Z*)-2-bromoethenyl)phenyl)nortropane (**4**, FP*m*ZBrENT),[70] along with the radiosynthesis and microPET imaging of [^{18}F]**1**-[^{18}F]**4** in anesthetized nonhuman primates and the PET imaging of [^{18}F]**1** in an awake nonhuman primate.

Chemistry

The synthesis of target compounds **1**−**4** is shown in Scheme 1. 2β-Carbomethoxy-3β-(3′-bromophenyl)tropane (**5**)[63] was hydrolyzed in refluxing 1,4-dioxane/H_2O[71] to give the acid **6** which was converted to the acid chloride and then esterified to afford the 2-fluoroethyl ester **7** or the 3-fluoropropyl ester **8**. *N*-demethylation[72] afforded the nortropanes **9** and **10**, which were coupled to (*Z*)-1,2-bis(trimethylstannyl)ethene[73,74] to give the vinyl−tin nortropanes **11** and **12** in varying cis/trans ratios with the major product being the cis isomer (∼3:1). Halodestannylation then afforded the vinyl iodides **1** and **3** and the vinyl bromides **2** and **4** (after separation of the cis/trans isomers by semipreparative HPLC).

Radiochemistry

The radiolabeling procedure is depicted in Scheme 2. *N*-Boc acid **13** or **14**[63] was dissolved in DMF, deprotonated with 0.1 M $Bu_4OH_{(aq)}$, added to [^{18}F]fluoroalkylbrosylate, and heated. The *N*-Boc group was cleaved under acidic conditions, the solution was neutralized, and the mixture was purified by semipreparative HPLC. The desired HPLC fractions were combined and the product was isolated by solid phase extraction according to a previously reported procedure.[75] We were able to obtain higher decay-corrected radiochemical yields with [^{18}F]FEtOBs than with [^{18}F]FPrOBs in our radiosyntheses (see Experimental Section). This is presumably because the carbon atom bonded to the brosylate leaving group bears a larger partial positive charge in [^{18}F]FEtOBs than [^{18}F]FPrOBs due to the electron-withdrawing properties of the fluorine atom which is two bonds away in [^{18}F]FEtOBs but three bonds away in [^{18}F]FPrOBs. The octanol/water partition coefficients[56−58] of [^{18}F]**1**−[^{18}F]**4** were measured according to a known procedure[76,77] and are shown in Table 1. These values are all in the range[56] that will allow for diffusion of the tracer across the blood-brain-barrier.

Table 1. Octanol/Water Partition Coefficients

compound	log $P_{7.4}$[a]	*n*
[^{18}F]**1**	1.69 ± 0.01	7
[^{18}F]**2**	1.40 ± 0.03	4
[^{18}F]**3**	1.64 ± 0.14	12
[^{18}F]**4**	1.87 ± 0.03	8

[a] Average value of *n* determinations ± the standard deviation.

In Vitro Competition Binding Assays

Vinylhalide nortropanes **1**−**4** and *trans*-**1** were screened for binding to human monoamine transporters using in vitro competition binding assays with transfected SERT, DAT, or NET according to our previously reported procedure.[61,78] The binding affinities for each transporter were determined using [^{3}H](*R*,*S*)-citalopram·HBr[78,79] ([^{3}H]**15**) (SERT), [^{125}I]RTI-55[80] (DAT), or [^{3}H]Nisoxetine[81] (NET). The data in Table 2 indicate that **1**−**4** all have a high affinity for the SERT and are selective for the SERT over the DAT and NET.[55] *trans*-**1** has a reduced affinity at all three transporters as expected based on previous reports.[60,74]

In Vivo Nonhuman Primate MicroPET Imaging

The in vivo regional brain uptake of [^{18}F]**1**−[^{18}F]**4** was determined in anesthetized cynomolgus monkeys (a total of 4 different cynomolgus monkeys) using a Concorde microPET P4 according to our previously reported procedure.[61] Baseline studies were initially performed to determine the extent of uptake of [^{18}F]**1**−[^{18}F]**4** in the SERT-rich regions of the brain. The baseline time-activity curves (TACs) for [^{18}F]**1** are shown in Figure 1. Compound [^{18}F]**1** enters the brain rapidly and achieves peak uptake in the SERT-rich brain regions after ∼ 45 min (Table S1, Supporting Information) with the highest uptake observed in the midbrain followed by the putamen, thalamus, medulla, and caudate. This rank order of uptake is similar to that observed with previously reported ^{11}C-labeled diarylsul-

Table 2. Results of In Vitro Competition Binding Assays with Transfected Human Monoamine Transporters

	K_i (nM)[a]			SERT selectivity	
compd	hSERT	hDAT	hNET	DAT/SERT	NET/SERT
1	0.43 ± 0.01[b]	87.6 ± 10.2[b]	109.9 ± 6.3[c]	~204	~256
2	0.33 ± 0.10[b]	35.5 ± 5.9[b]	101.3 ± 2.5[b]	~108	~307
3	0.26 ± 0.03[b]	179.7 ± 17.8[b]	67.5 ± 5.6[b]	~691	~260
4	0.33 ± 0.03[b]	118.7 ± 13.8[b]	30.2 ± 0.4[b]	~360	~92
trans-**1**	15.2 ± 3.9[b]	274.0 ± 9.3[b]	1180 ± 426[b]	~18	~78

[a] Average value of n determinations ± SEM (each determination performed in triplicate). [b] $n = 2$. [c] $n = 3$.

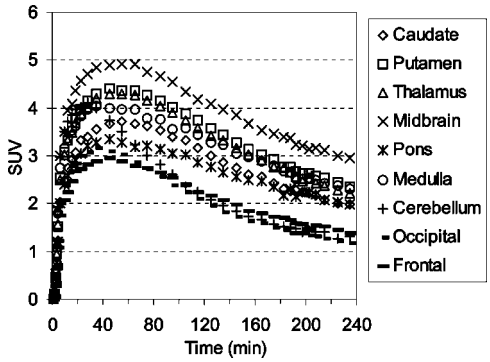

Figure 1. MicroPET baseline TACs obtained by injection of [^{18}F]**1** into an anesthetized cynomolgus monkey.

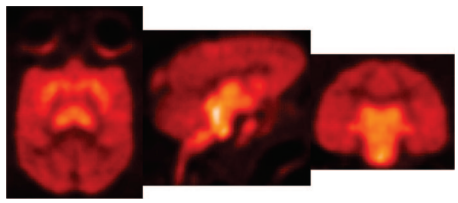

Figure 2. MicroPET images (summed 0−235 min) obtained by injection of [^{18}F]**1** into an anesthetized cynomolgus monkey.

fides[30,31,33,34,37] and is consistent with the known distribution of SERT in the brain.[34,59,82,83] Lesser uptake is observed in the pons and the occipital and frontal cortices. The uptake in the midbrain, putamen, thalamus, medulla, and caudate remains nearly constant for ~20 min (~45−65 min postinjection) and then begins to steadily wash out. In the cerebellum, a region with low SERT density,[59] peak uptake is achieved after ~27 min, followed by a rapid washout of radioactivity down to uptake levels similar to that observed in the occipital and frontal cortices. Between 65−175 min postinjection the washout from the SERT-rich brain regions remains nearly parallel with the washout from the cerebellum indicating that a quasi-equilibrium (a condition where the ratio of radioactivity uptake in the region of interest to reference region stays relatively constant)[37] has been established. The microPET images from this baseline study are shown in Figure 2.

Metabolite analysis of [^{18}F]**1** (Figure 3) was performed with arterial plasma samples and determined by an HPLC method with radioactivity detection as previously described.[61] The initial arterial plasma sample was taken at 1 min postinjection of [^{18}F]**1** and consisted of 93% of the total plasma radioactivity as unmetabolized [^{18}F]**1**. The percent of total plasma radioactivity then decreased over time during the course of the study to 13% unmetabolized [^{18}F]**1** after 180 min. The radioactive metabolite eluted immediately after the void volume during HPLC analysis and is believed to be [^{18}F]fluoroethanol (or one of its metabolic oxidation products [^{18}F]fluoroacetaldehyde or [^{18}F]fluoroacetic acid) that would result from hydrolysis of the [^{18}F]fluoroethyl ester.[84] The percentage of protein-bound [^{18}F]**1** in plasma at

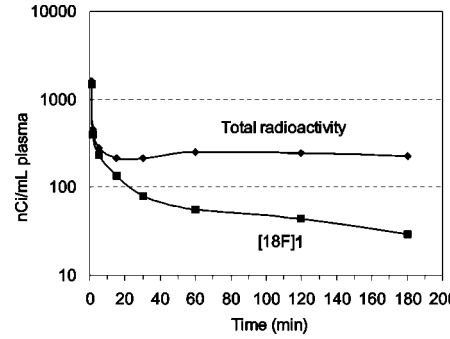

Figure 3. Metabolite analysis of [^{18}F]**1** in an anesthetized cynomolgus monkey.

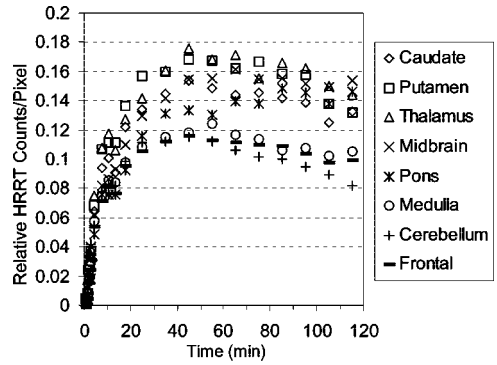

Figure 4. HRRT baseline TACs obtained by injection of [^{18}F]**1** into an awake rhesus monkey.

each time point is shown in Table S15, Supporting Information, and was in the range of 5.6−8.5% during the course of the study.

It has been previously shown that anesthesia during PET imaging can interfere with radioligand binding.[85−88] We therefore performed a baseline study in an awake rhesus monkey with [^{18}F]**1** using a Siemens/CTI High Resolution Research Tomograph (HRRT) to determine if there was a difference in the behavior of [^{18}F]**1** in an awake versus an anesthetized state. The TACs are shown in Figure 4 and the PET images are shown in Figure 5. High uptake is observed in the thalamus, putamen, midbrain, and caudate with peak uptake achieved after ~ 45 min (Table S2, Supporting Information). The behavior of [^{18}F]**1** in an awake monkey is very similar to its behavior in an anesthetized monkey thus demonstrating that the imaging properties of [^{18}F]**1** are not affected by anesthesia. We were not able to follow the washout of [^{18}F]**1** in the awake study for the same amount of time as with the anesthetized study because of the difficulty of keeping an awake monkey motionless for an extended period of time.

The TACs for the baseline studies with [^{18}F]**2**−[^{18}F]**4** are shown in Figures 6−8, respectively. Compound [^{18}F]**2** reaches peak uptake after 55−65 min in the SERT-rich brain regions followed by a steady washout (Table S3, Supporting Information). Peak uptake in the cerebellum is achieved after ~30 min,

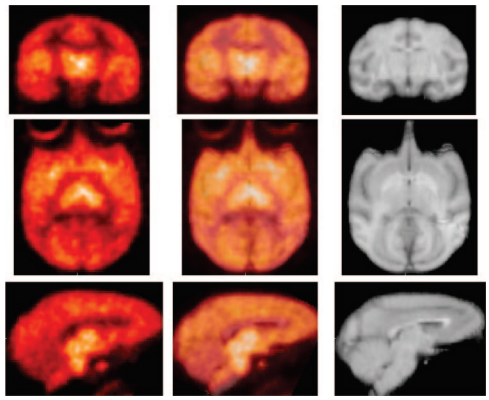

Figure 5. HRRT PET images (left, summed 60−120 min) obtained by injection of [^{18}F]**1** into an awake rhesus monkey. Composite MRI's of several rhesus monkeys (right) and overlaid images (center).

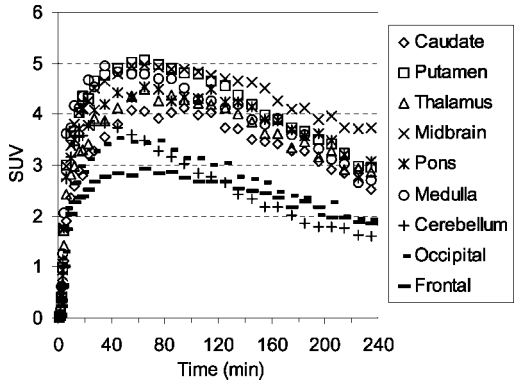

Figure 6. MicroPET baseline TACs obtained by injection of [^{18}F]**2** into an anesthetized cynomolgus monkey.

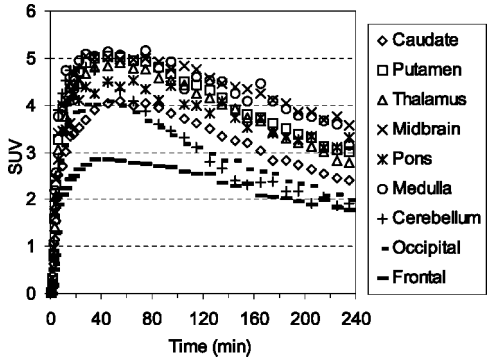

Figure 7. MicroPET baseline TACs obtained by injection of [^{18}F]**3** into an anesthetized cynomolgus monkey.

followed by a rapid washout to a level of uptake slightly less than that observed in the occipital and frontal cortices. Peak uptake in the SERT-rich brain regions for [^{18}F]**3** was achieved after 45−55 min (Table S4, Supporting Information) and for [^{18}F]**4** peak uptake was achieved after 35−45 min (Table S5, Supporting Information) with both compounds showing a steady washout. The ratio of uptake in the SERT-rich brain regions vs cerebellum uptake for compounds [^{18}F]**1**−[^{18}F]**4** at 115 and 215 min postinjection is shown in Table 3 (the complete data is shown in Tables S6−S10, Supporting Information, along with graphs of the uptake ratios versus time in Figures S1−S5, Supporting Information). The ratios for each tracer are very similar at these two time points thus indicating that these tracers all behave very similarly in vivo. The differences between the data in Table 3 are believed to be the result, at least partially,

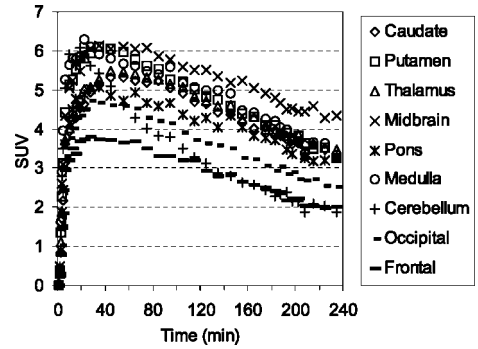

Figure 8. MicroPET baseline TACs obtained by injection of [^{18}F]**4** into an anesthetized cynomolgus monkey.

Table 3. Comparison of Uptake of [^{18}F]**1**−[^{18}F]**4** in SERT-Rich Brain Regions to Cerebellum Uptake at 115 and 215 min Post-Injection

brain region	115 min					215 min			
	[^{18}F]**1**[a]	[^{18}F]**1**	[^{18}F]**2**	[^{18}F]**3**	[^{18}F]**4**	[^{18}F]**1**	[^{18}F]**2**	[^{18}F]**3**	[^{18}F]**4**
caudate	1.6	1.4	1.5	1.2	1.4	1.5	1.6	1.2	1.7
putamen	1.6	1.7	1.7	1.4	1.5	1.8	1.8	1.5	1.7
thalamus	1.8	1.6	1.5	1.4	1.5	1.7	1.6	1.5	1.7
midbrain	1.9	1.9	1.7	1.5	1.7	2.2	2.1	1.8	2.2
pons	1.8	1.3	1.6	1.3	1.3	1.5	1.8	1.5	1.5
medulla	1.3	1.5	1.5	1.5	1.5	1.7	1.7	1.8	1.8
occipital	N/A	0.9	1.1	1.0	1.1	0.9	1.1	1.0	1.3
frontal	1.2	1.0	1.0	0.8	1.0	1.1	1.1	1.0	1.0

[a] HRRT awake rhesus study.

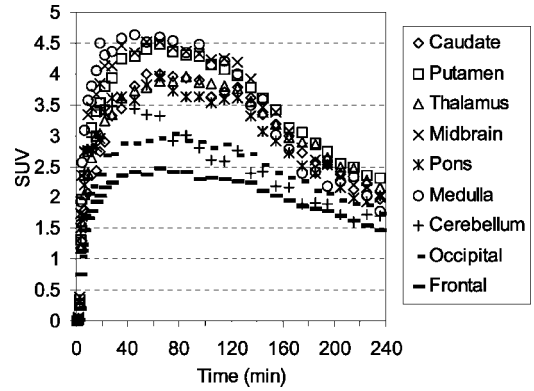

Figure 9. MicroPET TACs showing the results of injection of **15** (1.5 mg/kg) into an anesthetized cynomolgus monkey at 120 min postinjection of [^{18}F]**1**.

of individual differences between the monkeys studied rather than differences between the performance of each tracer. The uptake ratios for [^{18}F]**1** after 115 min in awake and anesthetized monkeys are also very similar which provides further evidence that isoflurane anesthesia does not influence the in vivo behavior of [^{18}F]**1**.

To demonstrate that the observed uptake in the baseline studies with [^{18}F]**1**−[^{18}F]**4** is the result of preferential binding to the SERT and not the DAT, chase studies were performed with the SERT ligand **15**, and the DAT ligands (±)-methylphenidate·HCl[89] (**16**) and RTI-113·HCl[71,90,91] (**17**). Figures 9−12 show the TACs for the chase studies with **15** at 120 min postinjection of the tracer for compounds [^{18}F]**1**-[^{18}F]**4**, respectively. For all four chase studies the amount of radioactivity in the SERT-rich brain regions decreases to nearly the level of the cortices and cerebellum thus indicating that the observed uptake is the result of binding to the SERT. These results also indicate that [^{18}F]**1**−[^{18}F]**4** can be used for occupancy studies of SERT-selective therapeutics.[26] Graphs of the uptake ratio

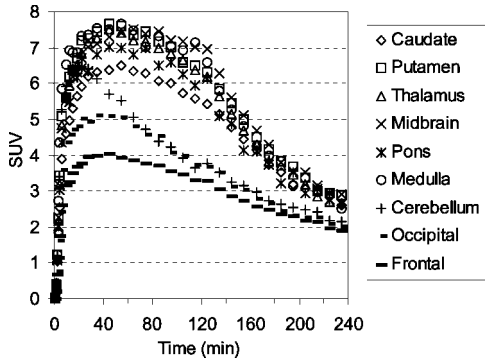

Figure 10. MicroPET TACs showing the results of injection of **15** (1.5 mg/kg) into an anesthetized cynomolgus monkey at 120 min postinjection of [^{18}F]**2**.

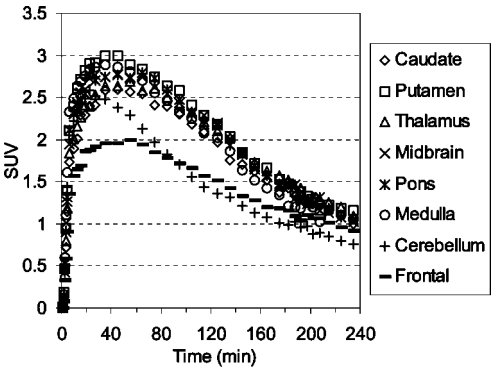

Figure 11. MicroPET TACs showing the results of injection of **15** (1.5 mg/kg) into an anesthetized cynomolgus monkey at 120 min postinjection of [^{18}F]**3**.

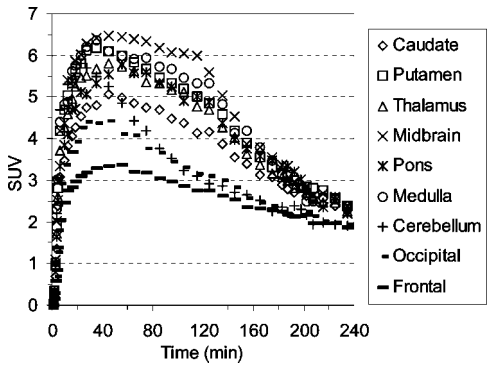

Figure 12. MicroPET TACs showing the results of injection of **15** (1.5 mg/kg) into an anesthetized cynomolgus monkey at 120 min postinjection of [^{18}F]**4**.

versus time for these chase studies are shown in Figures S6−S9, Supporting Information. Figure S10, Supporting Information, shows the results of chasing [^{18}F]**1** with the DAT ligand **16**, and Figure S11, Supporting Information, shows the results of chasing [^{18}F]**1** with the DAT ligand **17**. We chose to perform chase studies with both **16** and **17** because we wanted to chase [^{18}F]**1** with a tropane-based DAT ligand (**17**) and a nontropane-based DAT ligand (**16**). In neither case did the amount of radioactivity uptake decrease after administration of the chase compound (other than normal washout) thus indicating that [^{18}F]**1** is not bound to the DAT. Chase studies using **16** were also performed with [^{18}F]**2**-[^{18}F]**4** (Figures S12−S14, Supporting Information, respectively) and, similarly to what was observed with [^{18}F]**1**, the radioactivity was not displaced. We did not perform any chase studies with the NET ligand **18**[92,93]

Table 4. Comparison of the Times of Peak Uptake between [^{18}F]**1** and [^{18}F]**19** for Anesthetized and Awake Monkey Studies[a]

	time (min)			
	anesthetized		awake	
brain region	[^{18}F]**1**	[^{18}F]**19**	[^{18}F]**1**	[^{18}F]**19**
caudate	55	105	45	85
putamen	45	95	45	85
thalamus	45	85	45	>75
midbrain	45	95	45	>75
pons	45	115	85	>75
medulla	35	85	35	85
cerebellum	28	45	45	35

[a] See Tables S1, S2, S11, and S13, Supporting Information, for the complete data.

Table 5. Comparison of the Uptake Ratios between [^{18}F]**1** and [^{18}F]**19** for Anesthetized and Awake Monkey Studies at Selected Time Points[a]

	anesthetized						awake	
	55 min		115 min		225 min		95 min	
brain region	[^{18}F]**1**	[^{18}F]**19**	[^{18}F]**1**	[^{18}F]**19**	[^{18}F]**1**	[^{18}F]**19**	[^{18}F]**1**	[^{18}F]**19**
caudate	1.1	1.1	1.4	1.7	1.6	2.5	1.5	2.0
putamen	1.2	1.6	1.7	2.4	1.9	3.5	1.7	2.1
thalamus	1.2	1.5	1.6	2.2	1.8	3.1	1.7	2.4
midbrain	1.4	1.6	1.9	2.5	2.4	4.2	1.6	2.0
pons	0.9	1.2	1.3	2.0	1.6	3.1	1.5	1.6
medulla	1.1	1.5	1.5	2.1	1.9	3.0	1.1	1.5

[a] See Tables S6, S7, S12, and S14, Supporting Information, for the complete data. Also see Figures S1, S2, S16, and S18, Supporting Information.

because **18** also has an affinity for the SERT[60] and we have previously demonstrated that **18** will displace SERT PET tracers.[63,64]

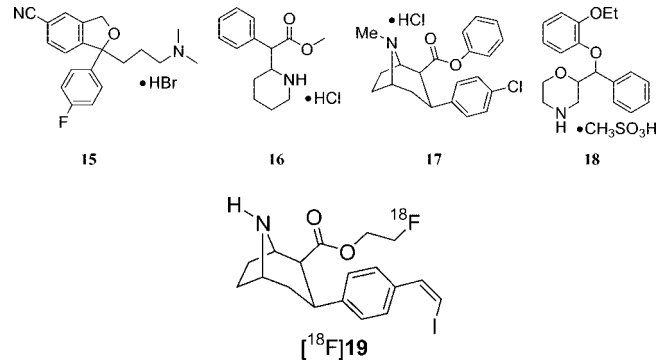

We have recently reported the microPET and HRRT PET imaging properties of [^{18}F]**19** in nonhuman primates (anesthetized and awake, respectively).[64] Compound **19** is the para-substituted isomer of **1** and has a higher affinity at all three transporters than **1** (K_i = 0.08 nM SERT, 13 nM DAT, and 28 nM NET) but a lower SERT versus DAT selectivity (~162). Comparison between [^{18}F]**19** and [^{18}F]**1** will reveal the effect of placing the vinyl iodide group in the para- or meta-position. The microPET baseline TACs for [^{18}F]**19** are reproduced in Figure S15, Supporting Information, and the awake rhesus monkey HRRT baseline TACs are reproduced in Figure S17, Supporting Information. Table 4 compares the times of peak uptake between [^{18}F]**19** and [^{18}F]**1** for the microPET and HRRT studies with each compound. In both the anesthetized and awake studies [^{18}F]**1** reaches peak uptake significantly faster than [^{18}F]**19** and [^{18}F]**1** also shows a greater washout (also see Tables S1, S2, S11, and S13, Supporting Information). Thus, [^{18}F]**1** has superior imaging kinetics relative to [^{18}F]**19**. Table 5 compares the ratio of uptake in SERT-rich brain regions to

cerebellum uptake for [^{18}F]**1** and [^{18}F]**19** (also see Tables S6, S7, S12, and S14, Supporting Information). Compound [^{18}F]**19** shows higher uptake ratios than [^{18}F]**1** in both anesthetized and awake states, and for both compounds the uptake ratios increase with time throughout the course of the studies (This is represented by Figures S1, S2, S16, and S18, Supporting Information, where the uptake ratio is plotted vs time). The differences in uptake ratio are a result of the differences in kinetics for each tracer. For compound [^{18}F]**1** (Figure 1) washout from the cerebellum begins after ~27 min and washout from the SERT-rich brain regions begins after ~65 min. This washout then remains fairly steady and the uptake ratios slowly increase until finally stabilizing after ~175 min (Figure S1, Supporting Information). In contrast, [^{18}F]**19** reaches peak uptake in the cerebellum after 45 min and then begins to wash out, while uptake in the SERT-rich brain regions continues to increase until 85−105 min followed by a very slow washout. This results in a continuously increasing uptake ratio with time (Figure S16, Supporting Information). Similar differences between [^{18}F]**1** and [^{18}F]**19** are also observed in the awake monkey studies (Figures S2 and S18, Supporting Information). Therefore, [^{18}F]**1** may be more ideally suited for measuring SERT density in humans because of its superior kinetics and the ability to achieve a quasi-equilibrium. Alternatively, as shown in Figure S19, Supporting Information, chasing [^{18}F]**19** with **15** produces a more drastic displacement of [^{18}F]**19** than occurs with [^{18}F]**1** (Figure 9) which suggests that [^{18}F]**19** may be better suited to be used for occupancy determination studies of SSRI's.[15,25−27] Thus, compounds [^{18}F]**1** and [^{18}F]**19** each have their own unique imaging properties and are both promising candidates for use in human PET studies. The decision of which tracer to use, [^{18}F]**1** or [^{18}F]**19**, would therefore have to be determined by the objective of the pending study.

Summary

The SERT ligands **1**−**4** were synthesized from *m*-bromophenyl tropane **5** and evaluated for binding to the SERT, DAT, and NET with in vitro competition binding assays using transfected cells. Compounds **1**−**4** have a high and nearly equal affinity for the SERT and are selective for the SERT over the DAT and NET. Radiolabeling afforded tracers [^{18}F]**1**−[^{18}F]**4** with higher decay-corrected radiochemical yields obtained with [^{18}F]FEtOBs than with [^{18}F]FPrOBs. Tracers [^{18}F]**1**−[^{18}F]**4** were found to have lipophilicities in the range log $P_{7.4}$ = 1.4−1.9. MicroPET imaging studies in anesthetized cynomolgus monkeys demonstrated that [^{18}F]**1**−[^{18}F]**4** behave very similarly in vivo with peak uptake achieved after 45−55 min, followed by a steady washout. The ratios of uptake in SERT-rich brain regions to cerebellum uptake for [^{18}F]**1**−[^{18}F]**4** were also very similar. An HRRT study was performed with [^{18}F]**1** in an awake rhesus monkey to determine if anesthesia was influencing the behavior of [^{18}F]**1**. The time to peak uptake and the uptake ratio of [^{18}F]**1** were similar between anesthetized and awake states indicating that anesthesia does not affect the imaging properties of [^{18}F]**1**. Chase studies with the SERT ligand **15** displaced tracers [^{18}F]**1**−[^{18}F]**4** but chase studies with the DAT ligand **16** did not displace tracers [^{18}F]**1**−[^{18}F]**4** thus indicating that the observed uptake in the brain is a result of preferential binding to the SERT and not the DAT. Comparison between [^{18}F]**1** and the para-substituted isomer [^{18}F]**19** demonstrates that the position of the vinyl iodide group can have a significant affect on the tracer properties of the two compounds. Peak uptake in the putamen and caudate is achieved after 45 and 55 min, respectively, with [^{18}F]**1** but it takes 95 and 105 min, respectively, with [^{18}F]**19**. Similar effects are observed in the midbrain and thalamus. Alternatively, the ratio of uptake in the SERT-rich brain regions to the cerebellum is higher with [^{18}F]**19** than with [^{18}F]**1**. Both [^{18}F]**1** and [^{18}F]**19** are, therefore, promising candidates for advancement to human studies because [^{18}F]**1** offers faster kinetics than [^{18}F]**19** but [^{18}F]**19** offers higher uptake ratios than [^{18}F]**1** and it will be interesting to see if these differences are maintained in human subjects. Additionally, each compound can be radiolabeled as [^{123}I]**1** or [^{123}I]**19** for SPECT imaging which will further expand the possible uses of these two tracers. We have, therefore, chosen to further pursue [^{18}F]**1** out of this series of tracers reported above in combination with [^{18}F]**19** due to the higher radiochemical yields that can be obtained by *O*-alkylation with [^{18}F]FEtOBs, the ability to use both [^{18}F]**1** and [^{18}F]**19** and to make direct comparisons between the two, and the possibility of radiolabeling each with ^{123}I for SPECT imaging. Thus, we intend to evaluate both [^{18}F]**1** and [^{18}F]**19** in healthy normal human volunteers under baseline conditions as well as perform test−retest variability in dose-dependent blocking studies to determine their suitability for measuring occupancy in subjects with neuropsychiatric disorders.

Experimental Section

General. Solvents were purchased from VWR and had originated from EMD or Burdick and Jackson. Anhydrous solvents (100-mL septum-capped bottles) were purchased from Aldrich. TLC plates used were EMD glass-backed Silica Gel 60 F_{254}, 20 × 20 cm, 250 μm. Preparatory TLC plates used were Analtech Uniplate Silica Gel GF 20 × 20 cm, 2000 μm. Silica gel used was EMD Silica Gel 60, 40−63 μm. Radial chromatography was performed with a Harrison Research Chromatotron. Semipreparatory HPLC: Waters XTerra Prep RP_{18}, 5 μm, 19 × 100 mm + guard cartridge (19 × 10 mm), 60:40:0.1 v/v/v MeOH/H_2O/NEt_3. Analytical HPLC: Waters NovaPak 3.9 × 150 mm, 75:25:0.1 v/v/v MeOH/H_2O/NEt_3. HRMS was performed by the Emory University Mass Spectrometry Center. NMR spectrometry was performed on Varian Inova and Unity spectrometers at the specified frequencies.

3β-(3′-Bromophenyl)tropane-2β-carboxylic acid (6). 2β-Carbomethoxy-3β-(3′-bromophenyl)tropane (**5**) (0.74 g, 2.19 mmol), 1,4-dioxane (15 mL), and H_2O (15 mL) were stirred at reflux for 16 h. The solvent was removed azeotropically with EtOH to give a white solid that was dried under vacuum for 3 h. The solid was suspended in $CHCl_3$ (5 mL), cooled to 0 °C, and the precipitate was isolated by filtration and dried under vacuum to afford 0.48 g (68%) of a white solid: ^{1}H NMR (600 MHz, CD_3OD) δ 7.51 (br s, 1 H), 7.36 (d, 1 H, J = 7.8 Hz), 7.31 (d, 1 H, J = 7.8 Hz), 7.20 (dd, 1 H, J = 7.8 Hz), 3.94 (m, 2 H), 3.36 (dt, 1 H, J = 6.0 Hz, J = 13.8 Hz), 2.81 (m, 1 H), 2.79 (s, 3 H), 2.69 (m, 1 H), 2.40 (m, 2 H), 2.17 (m, 2 H), 1.84 (m, 1 H); HRMS (APCI) $[MH]^+$ Calcd for $C_{15}H_{19}O_2N^{79}Br$ 324.0594, Found 324.0593; Calcd for $C_{15}H_{19}O_2N^{81}Br$ 326.0578, Found 326.0574.

2β-Carbo(2-fluoroethoxy)-3β-(3′-bromophenyl)tropane (7). 3β-(3′-Bromophenyl)tropane-2β-carboxylic acid (**6**) (0.43 g, 1.33 mmol) was suspended in anhydrous CH_2Cl_2 (25 mL) under Ar, followed by addition of anhydrous NEt_3 (0.30 mL, 2.15 mmol, 1.6 equiv.) and cooling to −4 °C. Oxalyl chloride (1.0 mL, 2 M CH_2Cl_2, 2.0 mmol, 1.5 equiv.) was diluted with anhydrous CH_2Cl_2 (5 mL) and added dropwise through the condenser to the reaction flask over a period of 5 min. The reaction mixture was stirred under Ar at −4 °C for 20 min, warmed to rt, and the solvent was removed to give a brown solid that was dried under vacuum for 20 min. The solid was dissolved in anhydrous CH_2Cl_2 (25 mL) and cooled to −4 °C under Ar. FEtOH (0.80 mL, 13.62 mmol 10.2 equiv.) and anhydrous NEt_3 (0.30 mL, 2.15 mmol, 1.6 equiv) were dissolved in anhydrous CH_2Cl_2 (10 mL) and added dropwise through the condenser to the acid chloride solution over a period of 3 min. The reaction mixture was stirred under Ar at −4 °C for 5 min, warmed to rt, and stirred at rt for 80 min, and then the solvent was removed to give a brown solid that was dried under

vacuum for 20 min. The solid was dissolved in CH_2Cl_2, poured onto dry silica (43 mm h × 43 mm i.d.), and eluted under vacuum: CH_2Cl_2 (100 mL), v/v/v hexane/EtOAc/NEt_3 75:20:5 (300 mL), 50:45:5 (100 mL) to afford 0.31 g (63%) of a colorless syrup: TLC R_f = 0.38 (50:45:5 v/v/v hexane/EtOAc/NEt_3); ^{1}H NMR (600 MHz, $CDCl_3$) δ 7.39 (s, 1 H), 7.29 (d, 1 H, J = 7.8 Hz), 7.21 (d, 1 H, J = 7.8 Hz), 7.14 (dd, 1 H, J = 7.8 Hz), 4.45 (dddd, 2 H, $^2J_{HF}$ = 46.8 Hz, $^3J_{HH}$ = 5.8 Hz, $^3J_{HH}$ = 2.6 Hz), 4.29 (dddd, 1 H, $^3J_{HF}$ = 29.4 Hz, $^2J_{HH}$ = 13.2 Hz, $^3J_{HH}$ = 5.2 Hz, $^3J_{HH}$ = 2.6 Hz), 4.08 (dddd, 1 H, $^3J_{HF}$ = 28.2 Hz, $^2J_{HH}$ = 12.6 Hz, $^3J_{HH}$ = 5.9 Hz, $^3J_{HH}$ = 2.4 Hz), 3.63 (m, 1 H), 3.36 (m, 1 H), 2.98 (m, 2 H), 2.53 (td, 1 H, J = 3.0 Hz, J = 12.3 Hz), 2.22 (s, 3 H), 2.20 (m, 1 H), 2.11 (m, 1 H), 1.70 (m, 2 H), 1.60 (m, 2 H); ^{13}C NMR (150 MHz, $CDCl_3$) δ 171.29, 145.79, 130.73, 129.69, 129.16, 126.10, 122.38, 81.74 (d, $^1J_{CF}$ = 169.2 Hz), 65.47, 62.91 (d, $^2J_{CF}$ = 20.6 Hz), 62.33, 52.65, 42.08, 34.04, 33.71, 25.95, 25.45; HRMS (APCI) $[MH]^+$ calcd for $C_{17}H_{22}O_2N^{79}Br$ 370.0813, found 370.0812; calcd for $C_{17}H_{22}O_2N^{81}Br$ 372.0797, found 372.0793.

2β-Carbo(3-fluoropropoxy)-3β-(3′-bromophenyl)tropane (8). 3β-(3′-Bromophenyl)tropane-2β-carboxylic acid (**6**) (0.11 g, 0.34 mmol) was suspended in anhydrous CH_2Cl_2 (8 mL) under Ar, followed by addition of anhydrous NEt_3 (0.08 mL, 0.57 mmol, 1.7 equiv.) and cooling to −4 °C. Oxalyl chloride (0.27 mL, 2 M CH_2Cl_2, 0.54 mmol, 1.6 equiv.) was diluted with anhydrous CH_2Cl_2 (2 mL) and added dropwise to the reaction flask over a period of 90 s. The reaction mixture was stirred under Ar at −4 °C for 20 min, warmed to rt, and the solvent was removed to give a brown solid that was dried under vacuum for 20 min. The solid was dissolved in anhydrous CH_2Cl_2 (10 mL) and cooled to −4 °C under Ar. FPrOH (0.32 g, 4.10 mmol 12.1 equiv.) and anhydrous NEt_3 (0.08 mL, 0.57 mmol, 1.7 equiv.) were dissolved in anhydrous CH_2Cl_2 (5 mL) and added dropwise to the acid chloride solution. The reaction mixture was stirred under Ar at −4 °C for 5 min, warmed to rt, and the solvent was removed to give a brown solid that was dried under vacuum for 10 min. The solid was dissolved in CH_2Cl_2, poured onto dry silica (39 mm h × 43 mm i.d.), and eluted under vacuum: CH_2Cl_2 (100 mL), v/v/v hexane/EtOAc/NEt_3 75:20:5 (300 mL), 50:45:5 (100 mL) to afford 88 mg (67%) of a colorless syrup: TLC R_f = 0.41 (50:45:5 v/v/v hexane/EtOAc/NEt_3); ^{1}H NMR (600 MHz, $CDCl_3$) δ 7.36 (s, 1 H), 7.29 (d, 1 H, J = 7.8 Hz), 7.19 (d, 1 H, J = 7.8 Hz), 7.14 (dd, 1 H, J = 7.8 Hz), 4.37 (2 m, 2 H, $^2J_{HF}$ = 47.1 Hz), 4.14 (m, 1 H), 3.98 (m, 1 H), 3.58 (m, 1 H), 3.35 (m, 1 H), 2.98 (dt, 1 H, J = 5.7 Hz, J = 12.0 Hz), 2.91 (m, 1 H), 2.50 (td, 1 H, J = 2.4 Hz, J = 12.6 Hz), 2.21 (s, 3 H), 2.18 (m, 1 H), 2.11 (m, 1 H), 1.85 (2 m, 2 H, $^3J_{HF}$ = 24.6 Hz), 1.70 (m, 2 H), 1.60 (m, 1 H); ^{13}C NMR (150 MHz, $CDCl_3$) δ 171.62, 146.01, 130.57, 129.72, 129.09, 125.98, 122.38, 80.89 (d, $^1J_{CF}$ = 165.0 Hz), 65.55, 62.29, 59.96 (d, $^3J_{CF}$ = 6.2 Hz), 52.80, 42.10, 34.11, 33.61, 29.94 (d, $^2J_{CF}$ = 20.6 Hz), 26.00, 25.43; HRMS (APCI) $[MH]^+$ Calcd for $C_{18}H_{24}O_2N^{79}BrF$ 384.0969, Found 384.0971; Calcd for $C_{18}H_{24}O_2N^{81}BrF$ 386.0954, Found 386.0953.

2β-Carbo(2-fluoroethoxy)-3β-(3′-bromophenyl)nortropane (9). 2β-Carbo(2-fluoroethoxy)-3β-(3′-bromophenyl)tropane (**7**) (0.26 g, 7.02 × 10^{-4} mol), 2,2,2-trichloroethyl chloroformate (1.0 mL, 7.27 mmol, 10.4 equiv.), $Na_2CO_{3(s)}$ (36 mg, 0.34 mmol, 0.5 equiv.), and toluene (15 mL) were stirred at reflux under Ar for 4 h, cooled, poured onto dry silica (43 mm h × 43 mm i.d.), and eluted under vacuum with CH_2Cl_2 (75 mL) and then 75:20:5 v/v/v/ hexane/EtOAc/NEt_3. The solvent was removed to give a colorless residue that was dried under vacuum (0.37 g). To the residue was added Zn dust (0.46 g), AcOH (10 mL), and H_2O (0.3 mL), and the mixture was stirred at rt for 21 h. The reaction mixture was filtered, the filtrate was diluted with CH_2Cl_2 (50 mL) and H_2O (50 mL), and cooled to 0 °C. The aqueous phase was basified to pH 11 with conc. $NH_4OH_{(aq)}$; the layers were separated, and the aqueous layer was extracted with CH_2Cl_2 (20 mL × 2). The combined CH_2Cl_2 layers were dried over $MgSO_4$, and the solvent was removed to give a colorless oil. The oil was dissolved in CH_2Cl_2, poured onto dry silica (35 mm h × 43 mm i.d.), and eluted under vacuum: CH_2Cl_2 (75 mL), then v/v/v hexane/EtOAc/NEt_3 75:20:5 (50 mL), 50:45:5 (50 mL), 20:75:5 (500 mL). The solvent was removed to give 0.18 g (72%) of a light yellow oil: TLC R_f = 0.10 (50:45:5 v/v/v hexane/EtOAc/NEt_3); ^{1}H NMR (600 MHz, $CDCl_3$) δ 7.35 (s, 1 H), 7.33 (m, 1 H), 7.15 (m, 2 H), 4.36 (dddd, 1 H, $^2J_{HF}$ = 46.8 Hz, $^2J_{HH}$ = 10.8 Hz, $^3J_{HH}$ = 2.4 Hz, $^3J_{HH}$ = 5.4 Hz), 4.23 (dddd, 1 H, $^2J_{HF}$ = 48.0 Hz, $^2J_{HH}$ = 10.8 Hz, $^3J_{HH}$ = 2.4 Hz, $^3J_{HH}$ = 6.6 Hz), 4.12 (dddd, 1 H, $^3J_{HF}$ = 26.4 Hz, $^2J_{HH}$ = 13.2 Hz, $^3J_{HH}$ = 2.4 Hz, $^3J_{HH}$ = 6.6 Hz), 4.01 (dddd, 1 H, $^3J_{HF}$ = 30.0 Hz, $^2J_{HH}$ = 13.2 Hz, $^3J_{HH}$ = 2.4 Hz, $^3J_{HH}$ = 5.4 Hz), 3.75 (m, 2 H), 3.25 (dt, 1 H, J = 6.0 Hz, J = 12.6 Hz), 2.82 (m, 1 H), 2.37 (td, 1 H, J = 3.0 Hz, J = 13.2 Hz), 2.12 (m, 1 H), 2.01 (m, 1 H), 1.76 (m, 1 H), 1.67 (m, 3 H); ^{13}C NMR (150 MHz, $CDCl_3$) δ 172.98, 144.85, 130.64, 130.00, 129.82, 126.21, 122.61, 81.25 (d, $^1J_{CF}$ = 169.2 Hz), 62.99 (d, $^2J_{CF}$ = 20.7 Hz), 56.54, 53.76, 51.08, 35.44, 33.60, 29.33, 27.89; HRMS (APCI) $[MH]^+$ Calcd for $C_{16}H_{20}O_2N^{79}BrF$ 356.0656, Found 356.0656; Calcd for $C_{16}H_{20}O_2N^{81}BrF$ 358.0635, Found 358.0636.

2β-Carbo(3-fluoropropoxy)-3β-(3′-bromophenyl)nortropane (10). 2β-Carbo(3-fluoropropoxy)-3β-(3′-bromophenyl)tropane (**8**) (78 mg, 2.03 × 10^{-4} mol), 2,2,2-trichloroethyl chloroformate (0.30 mL, 2.18 mmol, 10.7 equiv.), $Na_2CO_{3(s)}$ (11 mg, 0.10 mmol, 0.5 equiv.), and toluene (5 mL) were stirred at reflux under Ar for 4 h, cooled, poured onto dry silica (25 mm h × 33 mm i.d.), and eluted under vacuum with CH_2Cl_2 (25 mL) and then 75:20:5 v/v/v/ hexane/EtOAc/NEt_3 (100 mL). The solvent was removed to give a colorless residue that was dried under vacuum (0.11 g). To the residue was added Zn dust (0.13 g), AcOH (4 mL), and H_2O (0.1 mL), and the mixture was stirred at rt for 21 h. The reaction mixture was filtered; the filtrate was diluted with CH_2Cl_2 (25 mL) and H_2O (25 mL) and cooled to 0 °C. The aqueous phase was basified to pH 10 with conc. $NH_4OH_{(aq)}$; the layers were separated, and the aqueous layer was extracted with CH_2Cl_2 (10 mL × 2). The combined CH_2Cl_2 layers were dried over $MgSO_4$ and the solvent was removed to give a colorless oil. The oil was dissolved in CH_2Cl_2, poured onto dry silica (26 mm h × 33 mm i.d.), and eluted under vacuum: CH_2Cl_2 (75 mL), then v/v/v hexane/EtOAc/NEt_3 75:20:5 (50 mL), 50:45:5 (75 mL), 20:75:5 (100 mL). The solvent was removed to give 44 mg (59%) of a light yellow oil: ^{1}H NMR (600 MHz, $CDCl_3$) δ 7.33 (m, 2 H), 7.15 (m, 2 H), 4.17 (ddd, 2 H, $^2J_{HF}$ = 47.4 Hz, J_{HH} = 5.7 Hz), 4.01 (m, 1 H), 3.91 (m, 1 H), 3.73 (m, 2 H), 3.24 (dt, 1 H, J = 5.9 Hz, J = 13.2 Hz), 2.73 (d, 1 H, J = 5.4 Hz), 2.36 (td, 1 H, J = 2.4 Hz, J = 13.2 Hz), 2.13 (m, 1 H), 2.02 (m, 1 H), 1.69 (m, 6 H); ^{13}C NMR (150 MHz, $CDCl_3$) δ 173.30, 144.95, 130.74, 130.04, 129.83, 126.21, 122.61, 80.46 (d, $^1J_{CF}$ = 165.2 Hz), 60.11 (d, $^3J_{CF}$ = 5.9 Hz), 56.45, 53.67, 51.00, 35.62, 33.56, 29.68 (d, $^2J_{CF}$ = 20.7 Hz), 29.22, 27.79; HRMS (APCI) $[MH]^+$ Calcd for $C_{17}H_{22}O_2N^{79}BrF$ 370.0813, Found 370.0814; Calcd for $C_{17}H_{22}O_2N^{81}BrF$ 372.0792, Found 372.0793.

(*Z*)-1,2-Bis(trimethylstannyl)ethane. Purified acetylene (passed successively through a −78 °C cold trap, conc. $H_2SO_{4(aq)}$, $NaOH_{(s)}$, $CaCl_{2(s)}$, and then Drierite) was bubbled through a solution of hexamethylditin (2.52 g, 7.69 mmol), $Pd(PPh_3)_4$ (0.89 g, 0.77 mmol), and 1,4-dioxane (20 mL, purged with Ar for 45 min prior to use) at 65 °C for 4 h. The solution was cooled to rt, stirred at rt for 20 min, and filtered. The filtrate was poured onto silica gel (14 cm high × 4 cm i.d.) that had been pretreated with 10% NEt_3/hexane (100 mL) and then 1% NEt_3/hexane (100 mL). The product was eluted under vacuum with 1% NEt_3/hexane (200 mL), and the solvent was removed to give a dark orange oil that was briefly dried under vacuum (2.48 g, 91%). TLC R_f = 0.66 (1% NEt_3/Hexane); ^{1}H NMR (400 MHz, $CDCl_3$) δ 7.33 (s, 2 H), 0.17 (t, 18 H, $^2J_{SnH}$ = 26.6 Hz); ^{13}C NMR (150 MHz, $CDCl_3$) δ 155.17, −8.10.

(*Z*)-1,2-Bis(trimethylstannyl)ethene was found to be stable (by ^{1}H NMR spectroscopy) for at least 1 year when stored at −15 °C under Ar and protected from moisture and light (the vial was flushed with Ar, capped, wrapped with Parafilm, completely wrapped in Al foil, and then stored in a resealable plastic bag in a freezer).

2β-Carbo(2-fluoroethoxy)-3β-(3′-((*Z*)-2-trimethylstannylethenyl)phenyl)nortropane (11). 2β-Carbo(2-fluoroethoxy)-3β-(3′-bromophenyl)nortropane (**9**) (0.23 g, 6.46 × 10^{-4} mol), (*Z*)-1,2-bis(trimethylstannyl)ethene (0.72 g, 2.04 mmol, 3.2 equiv), $Pd(PPh_3)_4$ (80 mg, 6.92 × 10^{-5} mol, 0.1 equiv), and toluene (25

mL, purged with Ar for 2 h) were stirred at reflux under Ar for 18 h. The reaction mixture was cooled to rt, stirred at rt for 1.5 h, poured onto dry silica (40 mm h × 43 mm i.d.), and eluted under vacuum: CH_2Cl_2 (100 mL), hexane (50 mL), v/v/v hexane/EtOAc/NEt_3 75:20:5 (100 mL), 50:45:5 (100 mL), 20:75:5 (300 mL). The solvent was removed to give an orange oil that was radially chromatographed (4 mm silica, v/v/v hexane/EtOAc/NEt_3 90:8:2 (300 mL), 75:20:5 (1 L)) to afford 0.13 g of a colorless syrup that was ∼73:27 *cis/trans* by integration of the ^{1}H NMR vinyl resonances. The product was again radially chromatographed (2 mm silica, v/v/v hexane/EtOAc/NEt_3 95:4:1 (1 L), 90:8:2 (800 mL), 75:20:5 (200 mL), 50:45:5 (200 mL)) to afford 64 mg (21%) of a colorless syrup that was ∼93:7 *cis/trans*, 29 mg (10%) of a colorless syrup that was ∼76:24 *cis/trans*, and 29 mg (10%) of a colorless syrup that was ∼47:53 *cis/trans*. TLC R_f = 0.28 (20:75:5 v/v/v hexane/EtOAc/NEt_3); ^{1}H NMR (600 MHz, $CDCl_3$) δ 7.54 (td, 1 H, $^3J_{HH}$ = 13.8 Hz, $^3J_{SnH}$ = 75.0 Hz), 7.23 (dd, 1 H, J = 7.8 Hz), 7.11 (m, 3 H), 6.18 (td, 1 H, $^3J_{HH}$ = 13.8 Hz, $^2J_{SnH}$ = 32.0 Hz), 4.33 (dddd, 1 H, $^2J_{HF}$ = 46.9 Hz, $^2J_{HH}$ = 10.8 Hz, $^3J_{HH}$ = 5.4 Hz, $^3J_{HH}$ = 2.4 Hz), 4.20 (dddd, 1 H, $^2J_{HF}$ = 47.7 Hz, $^2J_{HH}$ = 10.8 Hz, $^3J_{HH}$ = 6.9 Hz, $^3J_{HH}$ = 2.4 Hz), 4.10 (partially resolved dddd, 1 H, $^3J_{HH}$ = 2.4 Hz), 3.95 (dddd, 1 H, $^3J_{HF}$ = 30.1 Hz, $^2J_{HH}$ = 13.0 Hz, $^3J_{HH}$ = 5.4 Hz, $^3J_{HH}$ = 2.4 Hz), 3.74 (m, 2 H), 3.27 (dt, 1 H, J = 5.4 Hz, J = 13.2 Hz), 2.83 (m, 1 H), 2.43 (td, 1 H, J = 3.0 Hz, J = 12.9 Hz), 2.13 (m, 1 H), 2.02, (m, 1 H), 1.77 (m, 1 H), 1.68 (m, 2 H), 1.61 (br s, 1 H), 0.08 (t, 9 H, $^2J_{SnH}$ = 27.3 Hz); ^{13}C NMR (100 MHz, $CDCl_3$) δ 173.18, 147.41, 142.29, 141.13, 133.71, 128.30, 126.86, 126.47, 125.57, 81.22 (d, $^1J_{CF}$ = 169.1 Hz), 62.85 (d, $^2J_{CF}$ = 20.5 Hz), 56.53, 53.84, 51.24, 35.75, 33.84, 29.37, 27.88, −7.89; HRMS (ESI) $[M + H]^+$ Calcd for $C_{21}H_{31}O_2NF^{120}Sn$ 468.1355, Found 468.1354.

2β-Carbo(3-fluoropropoxy)-3β-(3′-((*Z*)-2-trimethylstannylethenyl)phenyl)nortropane (12). 2β-Carbo(3-fluoropropoxy)-3β-(3′-bromophenyl)nortropane (**10**) (0.15 g, 4.05 × 10^{-4} mol), (*Z*)-1,2-bis(trimethylstannyl)ethene (0.54 g, 1.53 mmol, 3.8 equiv), $Pd(PPh_3)_4$ (73 mg, 6.32 × 10^{-5} mol, 0.16 equiv), and toluene (15 mL) were stirred at reflux under Ar for 16 h. The reaction mixture was cooled to rt, poured onto dry silica (40 mm h × 43 mm i.d.) that had been pretreated with 10% NEt_3/hexane (50 mL), and eluted under vacuum: CH_2Cl_2 (50 mL), hexane/EtOAc/NEt_3 v/v/v 75:20:5 (50 mL), 50:45:5 (50 mL), 20:75:5 (400 mL). The solvent was removed to give a brown oil (0.17 g) that was ∼78:22 cis/trans (+ impurities) by integration of the ^{1}H NMR vinyl resonances. Purification by radial chromatography (2 mm silica, v/v/v hexane/EtOAc/NEt_3 95:4:1 (100 mL), 90:8:2 (700 mL), 85:12:3 (100 mL), 80:16:4 (100 mL), and 75:20:5 (300 mL)) afforded 52 mg (27%) of a faint yellow syrup that was ∼91:9 cis/trans and 41 mg (21%) of a faint yellow syrup that was ∼68:32 cis/trans. TLC R_f = 0.24 (silica, 20:75:5 v/v/v hexane/EtOAc/NEt_3); ^{1}H NMR (600 MHz, $CDCl_3$) δ 7.52 (td, 1 H, $^3J_{HH}$ = 13.8 Hz, $^3J_{SnH}$ = 73.4 Hz), 7.22 (dd, 1 H, J = 7.5 Hz), 7.10 (s, 1 H), 7.08 (m, 2 H), 6.17 (td, 1 H, $^3J_{HH}$ = 13.8 Hz, $^2J_{SnH}$ = 32.1 Hz), 4.17 and 4.09 (dm, 1 H + 1 H, $^2J_{HF}$ = 46.8 Hz), 3.92 (m, 2 H), 3.73 (m, 1 H), 3.70 (m, 1 H), 3.25 (dt, 1 H, J = 5.9 Hz, J = 13.2 Hz), 2.73 (m, 1 H), 2.62 (br s, 1 H, NH − conc. dependent), 2.41 (td, 1 H, J = 13.2 Hz, J = 2.6 Hz), 2.11 (m, 1 H), 2.02 (m, 1 H), 1.76−1.58 (m, 5 H), 0.08 (t, 9 H, $^2J_{SnH}$ = 27.0 Hz); ^{13}C NMR (150 MHz, $CDCl_3$) δ 173.53, 147.32, 142.42, 141.09, 133.71, 128.35, 126.86, 126.50, 125.69, 80.53 (d, $^1J_{CF}$ = 165.5 Hz), 59.97 (d, $^3J_{CF}$ = 6.2 Hz), 56.52, 53.79, 51.20, 35.97, 33.90, 29.68 (d, $^2J_{CF}$ =19.9 Hz), 29.33, 27.86, −7.84; HRMS (ESI) $[M + H]^+$ Calcd for $C_{22}H_{33}O_2NF^{120}Sn$ 482.1512, found 482.1513.

2β-Carbo(2-fluoroethoxy)-3β-(3′-((*Z*)-2-iodoethenyl)phenyl)-nortropane (1). 2β-Carbo(2-fluoroethoxy)-3β-(3′-((*Z*)-2-trimethylstannylethenyl)phenyl)nortropane (**11**) (∼96:4 cis/trans, 35 mg, 7.51 × 10^{-5} mol) was dissolved in $CHCl_3$ (5 mL) and cooled to −2 °C under Ar. ICl (0.11 mL, 1.0 M CH_2Cl_2, 0.11 mmol, 1.5 equiv) was added dropwise, the reaction mixture was stirred at −2 °C under Ar for 15 min, and quenched by addition of $Na_2S_2O_3 \cdot 5H_2O$ (0.307 g, 1.24 mmol, in 5 mL H_2O). The mixture was diluted with $CHCl_3$ (5 mL) and H_2O (5 mL); the layers were separated, and the aqueous phase extracted with $CHCl_3$ (5 mL × 2). The combined $CHCl_3$ layers were dried over $MgSO_4$, the solvent was removed, and the residue was purified by preparative TLC (20:75:5 v/v/v hexane/EtOAc/NEt_3 × 2) to give 23 mg (71%) of a colorless residue that was ∼95:5 cis/trans by integration of the ^{1}H NMR vinyl resonances. Separation of the isomers by semipreparative HPLC (cis t_R = 19.7 min, 8.8 mL/min) afforded 16 mg (50%) of **1** as a white residue: ^{1}H NMR (600 MHz, $CDCl_3$) δ 7.47 and 7.46 (overlapping resonances, 2 H), 7.30 (m, 2 H), 7.20 (d, 1 H, J = 7.8 Hz), 6.56 (d, 1 H, J = 8.4 Hz), 4.31 (dddd, 1 H, $^2J_{HF}$ = 47.1 Hz, $^2J_{HH}$ = 10.6 Hz, $^3J_{HH}$ = 5.2 Hz, $^3J_{HH}$ = 2.4 Hz), 4.20 (partially resolved ddd, 0.5 H, $^2J_{HH}$ = 10.6 Hz, $^3J_{HH}$ = 7.1 Hz, $^3J_{HH}$ = 2.4 Hz), 4.11 (overlapping resonances, 0.5 H + 0.5 H, $^3J_{HH}$ = 2.4 Hz), 4.06 (ddd, 0.5 H, $^2J_{HH}$ = 12.9 Hz, $^3J_{HH}$ = 7.1 Hz, $^3J_{HH}$ = 2.4 Hz), 3.97 (dddd, 1 H, $^3J_{HF}$ = 30.3 Hz, $^2J_{HH}$ = 12.9 Hz, $^3J_{HH}$ = 5.2 Hz, $^3J_{HH}$ = 2.4 Hz), 3.77 (m, 2 H), 3.32 (dt, 1 H, J = 6.0 Hz, J = 12.6 Hz), 2.88 (m, 1 H), 2.44 (td, 1 H, J = 13.2 Hz, J = 3.0 Hz), 2.14 (m, 1 H), 2.03 (m, 1 H), 1.80 (m, 1 H), 1.71 (overlapping m + br s, 2 H + 1 H); ^{13}C NMR (150 MHz, $CDCl_3$) δ 172.90, 141.59, 138.68, 136.93, 128.37, 127.55, 127.45, 126.93, 81.26 (d, $^1J_{CF}$ = 170.1 Hz), 79.79, 63.26 (d, $^2J_{CF}$ = 18.7 Hz), 56.27, 53.91, 50.76, 35.28, 32.84, 28.71, 27.31; HRMS (ESI) $[MH]^+$ calcd for $C_{18}H_{22}O_2NF^{127}I$ 430.0674, found 430.0660.

***trans*-1.** ^{1}H NMR (600 MHz, $CDCl_3$) δ 7.40 (d, 1 H, J = 15.0 Hz), 7.24 (dd, 1 H, J = 7.8 Hz), 7.14 (s, 1 H), 7.13 (m, 2 H), 6.82 (d, 1 H, J = 15.0 Hz), 4.31 (dddd, 1 H, $^2J_{HF}$ = 47.2 Hz, $^2J_{HH}$ = 10.7 Hz, $^3J_{HH}$ = 5.5 Hz, $^3J_{HH}$ = 2.4 Hz), 4.19 (partially resolved ddd, 0.5 H, $^2J_{HH}$ = 10.7 Hz, $^3J_{HH}$ = 6.7 Hz, $^3J_{HH}$ = 2.4 Hz), 4.11 (overlapping resonances, 0.5 H + 0.5 H, $^3J_{HH}$ = 2.4 Hz), 4.06 (ddd, 0.5 H, $^2J_{HH}$ = 12.9 Hz, $^3J_{HH}$ = 6.7 Hz, $^3J_{HH}$ = 2.4 Hz), 3.95 (dddd, 1 H, $^3J_{HF}$ = 30.1 Hz, $^2J_{HH}$ = 12.9 Hz, $^3J_{HH}$ = 5.5 Hz, $^3J_{HH}$ = 2.4 Hz), 3.77 (m, 2 H), 3.27 (dt, 1 H, J = 12.6 Hz, J = 6.0 Hz), 2.83 (m, 1 H), 2.62 (br s, 1 H, NH), 2.41 (td, 1 H, J = 12.9 Hz, J = 3.0 Hz), 2.15 (m, 1 H), 2.04 (m, 1 H), 1.78 (m, 1 H), 1.68 (m, 2 H); semipreparative HPLC (t_R = 26.9 min, 8.8 mL/min).

2β-Carbo(2-fluoroethoxy)-3β-(3′-((*Z*)-2-bromoethenyl)phenyl)-nortropane (2). 2β-Carbo(2-fluoroethoxy)-3β-(3′-((*Z*)-2-trimethylstannylethenyl)phenyl)nortropane (**11**) (∼80:20 cis/trans, 38 mg, 8.15 × 10^{-5} mol) was dissolved in CH_2Cl_2 (4 mL) and cooled to 0 °C under Ar. Br_2 (35 mg, 0.22 mmol) was dissolved in CH_2Cl_2 (1 mL) and added dropwise until a faint yellow color remained. The reaction mixture was stirred at 0 °C under Ar for 6 min and then quenched by addition of $Na_2S_2O_3 \cdot 5H_2O$ (0.57 g in 4 mL H_2O). The reaction mixture was diluted by addition of CH_2Cl_2 (10 mL) and H_2O (10 mL), the layers were separated, and the aqueous layer was extracted with CH_2Cl_2 (5 mL × 2). The combined CH_2Cl_2 layers were dried over $MgSO_4$ and the solvent was removed to give a colorless residue that was purified by preparative TLC (silica, 20:75:5 v/v/v hexane/EtOAc/NEt_3) to afford 21 mg (67%) of a colorless residue that was ∼91:9 cis/trans by integration of the ^{1}H NMR vinyl resonances. The isomers were separated by semipreparative HPLC (9 mL/min, cis t_R = 15.9 min, trans t_R = 20.4 min) to afford 16 mg (51%) of **2** as a colorless residue: ^{1}H NMR (600 MHz, $CDCl_3$) δ 7.53 (d, 1 H, J = 7.8 Hz), 7.49 (s, 1 H), 7.30 (dd, 1 H, J = 7.8 Hz), 7.18 (d, 1 H, J = 7.2 Hz), 7.04 (d, 1 H, J = 8.4 Hz), 6.42 (d, 1 H, J = 7.8 Hz), 4.30 (dddd, 1 H, $^2J_{HF}$ = 47.1 Hz, $^2J_{HH}$= 10.7 Hz,$^3J_{HH}$= 2.4 Hz, $^3J_{HH}$= 5.3 Hz), 4.15 (unresolved dddd, 1 H, $^2J_{HF}$ = 47.1 Hz, $^2J_{HH}$ = 2.4 Hz), 4.09 (unresolved dddd, 1 H, $^2J_{HH}$ = 2.4 Hz), 3.96 (dddd, 1 H, $^3J_{HF}$ = 30.6 Hz, $^2J_{HH}$= 12.9 Hz,$^3J_{HH}$= 2.4 Hz, $^3J_{HH}$= 5.3 Hz), 3.82 (br s, 1 H), 3.31 (dt, 1 H, J = 6.0 Hz, J = 13.2 Hz), 2.87 (m, 1 H), 2.45 (unresolved td, 1 H, J = 12.6 Hz), 2.19 (m, 1 H), 2.07 (m, 1 H), 1.80 (m, 1 H), 1.72 (m, 2 H); ^{13}C NMR (150 MHz, $CDCl_3$) δ 173.13, 142.03, 135.13, 132.51, 128.40, 128.10, 127.56, 127.47, 106.71, 81.27 (d, $^1J_{CF}$ = 169.2 Hz), 63.08 (d, $^2J_{CF}$ = 18.6 Hz), 56.42, 53.89, 51.00, 35.47, 33.31, 29.07, 27.64; Analytical HPLC (t_R = 4.4 min, 1 mL/min); HRMS (ESI) $[MH]^+$ Calcd for $C_{18}H_{22}O_2NF^{79}Br$ 382.0813, Found 382.0815; Calcd for $C_{18}H_{22}O_2NF^{81}Br$ 384.0792, Found 384.0796.

2β-Carbo(3-fluoropropoxy)-3β-(3′-((*Z*)-2-iodoethenyl)phenyl)-nortropane (3). 2β-Carbo(3-fluoropropoxy)-3β-(3′-((*Z*)-2-trimethylstannylethenyl)phenyl)nortropane (**12**) (∼ 95:5 cis/trans, 84 mg,

1.75×10^{-4} mol) was dissolved in $CHCl_3$ (10 mL) and cooled to −7 °C under $Ar_{(g)}$. ICl (0.27 mL, 1.0 M CH_2Cl_2, 0.27 mmol, 1.5 equiv.) was added dropwise, the reaction mixture was warmed to rt, stirred at rt for 10 min, and quenched by addition of $Na_2S_2O_3 \cdot 5H_2O$ (0.683 g, 2.75 mmol, in 10 mL H_2O). The reaction mixture was diluted with $CHCl_3$ (25 mL) and H_2O (25 mL), the layers were separated, and the aqueous layer was extracted with $CHCl_3$ (10 mL × 2). The combined $CHCl_3$ layers were dried over $MgSO_4$, and the solvent was removed to give a yellow residue (85 mg) that was purified on Waters silica Sep-Pak Classics (2 in series): loaded with CH_2Cl_2 (1 mL), eluted with CH_2Cl_2 (1 mL), then hexane/EtOAc/NEt_3 v/v/v 90:8:2 (2 mL), 75:20:5 (5 mL), 50:45:5 (10 mL), 20:75:5 (25 mL). The desired fractions were combined, and the solvent was removed to give 43 mg (55%) of a yellow oil that was ∼86:14 cis/trans by integration of the ^{1}H NMR vinyl resonances. The isomers were separated by semipreparative HPLC (8.8 mL/min; cis t_R = 25.2 min; trans t_R = 34.3 min) to afford 26 mg (34%) of **3** as an opaque residue: ^{1}H NMR (600 MHz, $CDCl_3$) δ 7.47 and 7.46 (overlapping resonances, 2 H, J = 8.4 Hz), 7.29 (m, 2 H), 7.18 (d, 1 H, J = 7.8 Hz), 6.56 (d, 1 H, J = 8.4 Hz), 4.14 (m, 1 H), 4.06 (m, 1 H), 3.98 (quintet, 1 H, J = 6.0 Hz), 3.87 (m, 1 H), 3.76 (m, 1 H), 3.73 (m, 1 H), 3.31 (dt, 1 H, J = 13.2 Hz, J = 5.4 Hz), 2.78 (d, 1 H, J = 5.4 Hz), 2.53 (br s, 1 H, NH), 2.43 (td, 1 H, J = 2.4 Hz, J = 12.9 Hz), 2.14 (m, 1 H), 2.03 (m, 1 H), 1.78 (m, 1 H), 1.68 (m, 3 H), 1.58 (m, 1 H); ^{13}C NMR (150 MHz, $CDCl_3$) δ 173.52, 142.47, 138.64, 136.79, 128.32, 127.63, 126.78, 80.55 (d, $^1J_{CF}$ = 165.0 Hz), 79.56, 59.97 (d, $^3J_{CF}$ = 4.5 Hz), 56.47, 53.75, 51.19, 35.73, 33.58, 29.70 (d, $^2J_{CF}$ = 20.6 Hz), 29.31, 27.83; HRMS (ESI) $[MH]^+$ Calcd for $C_{19}H_{24}O_2NF^{127}I$ 444.0830, found 444.0825.

2β-Carbo(3-fluoropropoxy)-3β-(3′-((*Z*)-2-bromoethenyl)phenyl)nortropane (4). 2β-Carbo(3-fluoropropoxy)-3β-(3′-((*Z*)-2-trimethylstannylethenyl)phenyl)nortropane (**12**) (∼ 91:9 cis/trans, 52 mg, 1.08×10^{-4} mol) was dissolved in $CHCl_3$ (5 mL) and cooled to 0 °C under Ar. Br_2 (58 mg, 3.63×10^{-4} mol, 3.4 equiv.) was dissolved in $CHCl_3$ (1 mL) and added dropwise until a faint yellow color persisted (not all of the solution was added). The reaction mixture was stirred at 0 °C under Ar for 15 min and then quenched by addition of $Na_2S_2O_3 \cdot 5\ H_2O$ (98 mg, 3.95×10^{-4} mol, dissolved in 10 mL H_2O). The mixture was diluted with $CHCl_3$ (10 mL) and H_2O (10 mL); the layers were separated, and the aqueous layer was extracted with $CHCl_3$ (10 mL × 2). The combined $CHCl_3$ layers were dried over $MgSO_4$, and the solvent was removed to give a colorless syrup that became an opaque residue when dried under vacuum. The residue was dissolved in CH_2Cl_2, poured onto dry silica (26 mm h × 33 mm i.d.), and eluted under vacuum: CH_2Cl_2 (25 mL), hexanes/EtOAc/NEt_3 v/v/v 75:20:5 (25 mL), 50:45:5 (50 mL), 20:75:5 (250 mL). The isolated product was further purified by preparative TLC (20:75:5 v/v/v hexanes/EtOAc/NEt_3) to give a faint yellow syrup (26 mg) that was ∼93:7 cis/trans by integration of the ^{1}H NMR vinyl resonances. The isomers were separated by semipreparative HPLC (cis t_R = 20.3 min, 9.0 mL/min) to afford 21 mg (49%) of a colorless residue: ^{1}H NMR (600 MHz, $CDCl_3$) δ 7.53 (d, 1 H, J = 7.2 Hz), 7.49 (s, 1 H), 7.30 (dd, 1 H, J = 7.2 Hz), 7.15 (d, 1 H, J = 7.2 Hz), 7.04 (d, 1 H, J = 8.4 Hz), 6.44 (d, 1 H, J = 8.4 Hz), 4.11 (m, 1 H), 4.03 (m, 1 H), 3.97 (quintet, 1 H, J = 5.9 Hz), 3.87 (m, 2 H), 3.82 (m, 1 H), 3.32 (dt, 1 H, J = 6.0 Hz, J = 12.6 Hz), 2.80 (overlapping resonances: br s + m, 2 H), 2.46 (td, 1 H, J = 2.4 Hz, J = 13.2 Hz), 2.25 (m, 1 H), 2.14 (m, 1 H), 1.82 (m, 1 H), 1.74 (m, 2 H), 1.65 (m, 1 H), 1.54 (m, 1 H); ^{13}C NMR (150 MHz, $CDCl_3$) δ 173.55, 141.61, 135.24, 132.32, 128.51, 128.11, 127.69, 127.51, 106.90, 80.41 (d, $^1J_{CF}$ = 166.0 Hz), 60.38 (d, $^3J_{CF}$ = 4.2 Hz), 56.31, 53.86, 50.64, 35.63, 33.00, 29.57 (d, $^2J_{CF}$ = 18.7 Hz), 28.63, 27.34; HRMS (ESI) $[M + H]^+$ Calcd for $C_{19}H_{24}O_2FN^{79}Br$ 396.0969, found 396.0974.

[^{18}F]Fluoroethylbrosylate. $H^{18}F$ was produced with a Siemens 11-MeV RDS 112 cyclotron by employing the $^{18}O(p,n)^{18}F$ reaction in $H_2{}^{18}O$. The $H^{18}F_{(aq)}$ was transferred to a chemical processing control unit (CPCU), collected on a trap/release cartridge, released with $K_2CO_{3(aq)}$ (0.9 mg in 0.6 mL H_2O), and added to a CH_3CN solution of Kryptofix 222 (5 mg in 1 mL). The solution was placed in a 110 °C oil bath, the solvent was evaporated under a $N_{2(g)}$ flow, and CH_3CN (3 mL) was added and evaporated in order to azeotropically dry the Kryptofix 222/ $K^{18}F$. 1,2-Dibrosylethane (4 mg in 1 mL CH_3CN) was added, the reaction mixture was heated at 90 °C for 10 min, and the [^{18}F]fluoroethylbrosylate was trapped on a Waters silica Sep-Pak Classic (WAT051900) (previously prepped with 10 mL EtOEt). The [^{18}F]fluoroethylbrosylate was eluted with EtOEt, the EtOEt solution was transferred to a hot cell under $N_{2(g)}$ pressure and collected in a V-tube to give [^{18}F]fluoroethylbrosylate in 74% radiochemical yield (decay corrected from transfer of $H^{18}F_{(aq)}$ to the CPCU). The V-tube was placed in an 80 °C oil bath and the EtOEt was evaporated with an $Ar_{(g)}$ flow. The solution of radiolabeling precursor was then added to this V-tube (see below).

[^{18}F]Fluoropropylbrosylate. Prepared in an analogous manner as [^{18}F]fluoroethylbrosylate using 1,3-dibrosylpropane.

2β-Carbo(2-[^{18}F]fluoroethoxy)-3β-(3′-((*Z*)-2-iodoethenyl)phenyl)nortropane ([^{18}F]1). *N*-(*t*-butoxycarbonyl)-3β-(3′-((*Z*)-2-iodoethenyl)phenyl)nortropane-2β-carboxylic acid (**13**) (∼ 1.1 mg, ∼98:2 cis/trans) was dissolved in DMF (0.3 mL), deprotonated by addition of 0.1 M $Bu_4NOH_{(aq)}$ (16 μL, 0.7 equiv), and added to [^{18}F]fluoroethylbrosylate. The solution was heated at 90 °C for 10 min, 6 M $HCl_{(aq)}$ (∼0.16 mL, ∼422 equiv) was added, the solution was heated at 90 °C for 10 min, cooled to 0 °C, and neutralized by addition of 6 M $NH_4OH_{(aq)}$ (∼0.16 mL, ∼422 equiv). The solution was diluted with HPLC solvent and purified by semipreparative HPLC (t_R (range) = 15−19 min, 9.2 mL/min). The desired fractions were combined, diluted 1:2 v/v with H_2O and loaded onto a Waters C_{18} Sep-Pak. The Sep-Pak was washed with 0.9% $NaCl_{(aq)}$ (40 mL) and then EtOH (0.5 mL). The product was eluted from the Sep-Pak with EtOH (1.5 mL) and collected in a sealed sterile vial containing 0.9% $NaCl_{(aq)}$ (3.5 mL). This solution was passed successively through a 1 μm filter and then a 0.2 μm filter (Acrodisc PTFE) under Ar-pressure and collected in a sealed sterile dose vial containing 0.9% $NaCl_{(aq)}$ (10 mL). The total synthesis time was ∼80 min from the delivery of [^{18}F]fluoroethylbrosylate to the hot cell with a 6.3 ± 1.8% (n = 4) radiochemical yield (decay corrected). The product was then analyzed by analytical HPLC (t_R = 4.9 min, 1 mL/min) to determine the radiochemical purity (97 ± 2%, n = 4).

2β-Carbo(2-[^{18}F]fluoroethoxy)-3β-(3′-((*Z*)-2-bromoethenyl)phenyl)nortropane ([^{18}F]2). *N*-(*t*-butoxycarbonyl)-3β-(3′-((*Z*)-2-bromoethenyl)phenyl)nortropane-2β-carboxylic acid (**14**) (∼0.6 mg, ∼95:5 cis/trans) was dissolved in DMF (0.3 mL), deprotonated by addition of 0.1 M $Bu_4NOH_{(aq)}$ (10 μL, 0.7 equiv), and added to [^{18}F]fluoroethylbrosylate. The solution was heated at 90 °C for 10 min, 6 M $HCl_{(aq)}$ (∼0.11 mL, ∼480 equiv) was added, the solution was heated at 90 °C for 10 min, cooled to 0 °C, and neutralized by addition of 6 M $NH_4OH_{(aq)}$ (∼0.11 mL, ∼480 equiv). The solution was diluted with HPLC solvent and purified by semipreparative HPLC (t_R (range) = 10−16 min, 9.2 mL/min). The desired fractions were combined, diluted 1:2 v/v with H_2O and loaded onto a Waters C_{18} Sep-Pak. The Sep-Pak was washed with 0.9% $NaCl_{(aq)}$ (40 mL) and then EtOH (0.5 mL). The product was eluted from the Sep-Pak with EtOH (1.5 mL) and collected in a sealed sterile vial containing 0.9% $NaCl_{(aq)}$ (3.5 mL). This solution was passed successively through a 1 μm filter and then a 0.2 μm filter (Acrodisc PTFE) under Ar-pressure and collected in a sealed sterile dose vial containing 0.9% $NaCl_{(aq)}$ (10 mL). The total synthesis time was ∼75 min from the delivery of [^{18}F]fluoroethylbrosylate to the hot cell with a 4.2 ± 2.7% (n = 3) radiochemical yield (decay corrected). The product was then analyzed by analytical HPLC (t_R = 4.4 min, 1 mL/min) to determine the radiochemical purity (95 ± 2%, n = 3).

2β-Carbo(3-[^{18}F]fluoropropoxy)-3β-(3′-((*Z*)-2-iodoethenyl)phenyl)nortropane ([^{18}F]3). *N*-(*t*-butoxycarbonyl)-3β-(3′-((*Z*)-2-iodoethenyl)phenyl)nortropane-2β-carboxylic acid (**13**) (∼0.6 mg) was dissolved in DMF (0.3 mL), deprotonated by addition of 0.1 M $Bu_4NOH_{(aq)}$ (11 μL, 0.9 equiv), and added to [^{18}F]fluoropropylbrosylate. The solution was heated at 105 °C for 10 min, and 6 M $HCl_{(aq)}$ (∼0.12 mL, ∼ 580 equiv) was added. The solution was

heated at 105 °C for 10 min, cooled to 0 °C, and neutralized by addition of 6 M $NH_4OH_{(aq)}$ (~0.12 mL, ~580 equiv). The solution was diluted with HPLC solvent and purified by semipreparative HPLC (t_R (range) = 21−25 min, 9.2 mL/min). The desired fractions were combined, diluted 1:2 v/v with H_2O, and loaded onto a Waters C_{18} Sep-Pak. The Sep-Pak was washed with 0.9% $NaCl_{(aq)}$ (40 mL) and then EtOH (0.5 mL). The product was eluted from the Sep-Pak with EtOH (1.5 mL) and collected in a sealed sterile vial containing 0.9% $NaCl_{(aq)}$ (3.5 mL). This solution was passed successively through a 1 μm filter and then a 0.2 μm filter (Acrodisc PTFE) under Ar-pressure and collected in a sealed sterile dose vial containing 0.9% $NaCl_{(aq)}$ (10 mL).

The total synthesis time was ~80 min from the delivery of [^{18}F]fluoropropylbrosylate to the hot cell with a 1.9 ± 0.8% (n = 3) radiochemical yield (decay corrected). The product was then analyzed by analytical HPLC (t_R = 6.3 min, 1 mL/min) to determine the radiochemical purity (94 ± 4%, n = 3).

2β-Carbo(3-[^{18}F]fluoropropoxy)-3β-(3′-((*Z*)-2-bromoethenyl)phenyl)nortropane ([^{18}F]4). *N*-(*t*-Butoxycarbonyl)-3β-(3′-((*Z*)-2-bromoethenyl)phenyl)nortropane-2β-carboxylic acid (**14**) (~0.6 mg) was dissolved in DMF (0.3 mL), deprotonated by addition of 0.1 M $Bu_4NOH_{(aq)}$ (12 μL, 0.9 equiv), and added to [^{18}F]fluoropropylbrosylate. The solution was heated at 90 °C for 10 min, 6 M $HCl_{(aq)}$ (~0.15 mL, ~ 655 equiv) was added, the solution was heated at 90 °C for 10 min, cooled to 0 °C, and neutralized by addition of 6 M $NH_4OH_{(aq)}$ (~0.15 mL, ~655 equiv). The solution was diluted with HPLC solvent and purified by semipreparative HPLC (t_R (range) = 15−20 min, 9.2 mL/min). The desired fractions were combined, diluted 1:2 v/v with H_2O and loaded onto a Waters C_{18} Sep-Pak. The Sep-Pak was washed with 0.9% $NaCl_{(aq)}$ (40 mL) and then EtOH (0.5 mL). The product was eluted from the Sep-Pak with EtOH (1.5 mL) and collected in a sealed sterile vial containing 0.9% $NaCl_{(aq)}$ (3.5 mL). This solution was passed successively through a 1 μm filter and then a 0.2 μm filter (Acrodisc PTFE) under Ar-pressure and collected in a sealed sterile dose vial containing 0.9% $NaCl_{(aq)}$ (10 mL). The total synthesis time was ~77 min from the delivery of [^{18}F]fluoropropylbrosylate to the hot cell with a 1.7 ± 0.3% (n = 3) radiochemical yield (decay corrected). The product was then analyzed by analytical HPLC (t_R = 6.0 min, 1 mL/min) to determine the radiochemical purity (93 ± 7%, n = 3).

Acknowledgment. This research was sponsored by the NIMH (1-R21-MH-66622-01). We acknowledge the use of shared instrumentation provided by grants from the NIH and the NSF.

Note Added after ASAP Publication. This manuscript was released ASAP on November 24, 2008 with incorrect labeling for the last two tables. The correct version was posted on December 18, 2008.

Supporting Information Available: Additional microPET data and elemental analysis data of **1**−**4**. This material is available free of charge via the Internet at http://pubs.acs.org.

References

(1) Thie, J. A. Understanding the Standardized Uptake Value, Its Methods, and Implications for Usage. *J. Nucl. Med.* **2004**, *45*, 1431–1434.
(2) Bentourkia, M.; Zaidi, H. Tracer Kinetic Modeling in PET. *PET Clin.* **2007**, *2*, 267–277.
(3) Rudnick, G. Active Transport of 5-Hydroxytryptamine by Plasma Membrane Vesicles Isolated from Human Blood Platelets. *J. Biol. Chem.* **1977**, *252*, 2170–2174.
(4) Blakely, R. D.; De Felice, L. J.; Hartzell, H. C. Molecular Physiology of Norepinephrine and Serotonin Transporters. *J. Exp. Biol.* **1994**, *196*, 263–281.
(5) Torres, G. E.; Gainetdinov, R. R.; Caron, M. G. Plasma Membrane Monoamine Transporters: Structure, Regulation and Function. *Nat. Rev. Neurosci.* **2003**, *4*, 13–25.
(6) Linder, A. E.; Ni, W.; Diaz, J. L.; Szasz, T.; Burnett, R.; Watts, S. W. Serotonin (5-HT) in Veins: Not All in Vain. *J. Pharmacol. Exp. Ther.* **2007**, *323*, 415–421.
(7) Owens, M. J.; Nemeroff, C. B. Role of Serotonin in the Pathophysiology of Depression: Focus on the Serotonin Transporter. *Clin. Chem.* **1994**, *40*, 288–295.
(8) Fujita, M.; Shimada, S.; Maeno, H.; Nishimura, T.; Tohyama, M. Cellular Localization of Serotonin Transporter mRNA in the Rat Brain. *Neurosci. Lett.* **1993**, *162*, 59–62.
(9) Austin, M. C.; Bradley, C. C.; Mann, J. J.; Blakely, R. D. Expression of Serotonin Transporter Messenger RNA in the Human Brain. *J. Neurochem.* **1994**, *62*, 2362–2367.
(10) Stockmeier, C. A.; Shapiro, L. A.; Haycock, J. W.; Thompson, P. A.; Lowy, M. T. Quantitative Subregional Distribution of Serotonin-1A Receptors and Serotonin Transporters in the Human Dorsal Raphe. *Brain Res.* **1996**, *727*, 1–12.
(11) Lucki, I. The Spectrum of Behaviors Influenced by Serotonin. *Biol. Psychiatry* **1998**, *44*, 151–162.
(12) Owens, M. J.; Nemeroff, C. B. The Serotonin Transporter and Depression. *Depression Anxiety* **1998**, *8*, 5–12.
(13) Mann, J. J. Role of the Serotonergic System in the Pathogenesis of Major Depression and Suicidal Behavior. *Neuropsychopharm.* **1999**, *21*, 99S–105S.
(14) Mann, J. J.; Brent, D. A.; Arango, V. The Neurobiology and Genetics of Suicide and Attempted Suicide: A Focus on the Serotonergic System. *Neuropsychopharm.* **2001**, *24*, 467–477.
(15) Laakso, A.; Hietala, J. PET Studies of Brain Monoamine Transporters. *Curr. Pharm. Des.* **2000**, *6*, 1611–1623.
(16) Laruelle, M.; Slifstein, M.; Huang, Y. Positron Emission Tomography: Imaging and Quantification of Neurotransporter Availability. *Methods* **2002**, *27*, 287–299.
(17) Ametamey, S. M.; Honer, M.; Schubiger, P. A. Molecular Imaging with PET. *Chem. Rev.* **2008**, *108*, 1501–1516.
(18) Benmansour, S.; Cecchi, M.; Morilak, D. A.; Gerhardt, G. A.; Javors, M. A.; Gould, G. G.; Frazer, A. Effects of Chronic Antidepressant Treatments on Serotonin Transporter Function, Density, and mRNA Level. *J. Neurosci.* **1999**, *19*, 10494–10501.
(19) Benmansour, S.; Owens, W. A.; Cecchi, M.; Morilak, D. A.; Frazer, A. Serotonin Clearance in vivo is Altered to a Greater Extent by Antidepressant-Induced Downregulation of the Serotonin Transporter than by Acute Blockade of this Transporter. *J. Neurosci.* **2002**, *22*, 6766–6772.
(20) Kugaya, A.; Sanacora, G.; Staley, J. K.; Malison, R. T.; Bozkurt, A.; Khan, S.; Anand, A.; van Dyck, C. H.; Baldwin, R. M.; Seibyl, J. P.; Charney, D.; Innis, R. B. Brain Serotonin Transporter Availability Predicts Treatment Response to Selective Serotonin Reuptake Inhibitors. *Biol. Psychiatry* **2004**, *56*, 497–502.
(21) Mirza, N. R.; Nielsen, E. Ø.; Troelsen, K. B. Serotonin Transporter Density and Anxiolytic-like Effects of Antidepressants in Mice. *Prog. Neuro-Psychopharm. Biol. Psych.* **2007**, *31*, 858–866.
(22) Meyer, J. H. Imaging the Serotonin Transporter During Major Depressive Disorder and Antidepressant Treatment. *J. Psychiatry Neurosci.* **2007**, *32*, 86–102.
(23) Aboagye, E. O.; Price, P. M.; Jones, T. In Vivo Pharmacokinetics and Pharmacodynamics in Drug Development Using Positron-Emission Tomography. *Drug Discovery Today* **2001**, *6*, 293–302.
(24) Guilloteau, D.; Chalon, S. PET and SPECT Exploration of Central Monoaminergic Transporters for the Development of New Drugs and Treatments in Brain Disorders. *Curr. Pharm. Design* **2005**, *11*, 3237–3245.
(25) Lee, C.-M.; Farde, L. Using Positron Emission Tomography to Facilitate CNS Drug Development. *Trends Pharmacol. Sci.* **2006**, *27*, 310–316.
(26) Takano, A.; Suzuki, K.; Kosaka, J.; Ota, M.; Nozaki, S.; Ikoma, Y.; Tanada, S.; Suhara, T. A Dose-Finding Study of Duloxetine Based on Serotonin Transporter Occupancy. *Psychopharmacology* **2006**, *185*, 395–399.
(27) Talbot, P. S.; Laruelle, M. The Role of In Vivo Molecular Imaging with PET and SPECT in the Elucidation of Psychiatric Drug Action and New Drug Development. *Eur. Neuropsychopharmacol.* **2002**, *12*, 503–511.
(28) Hargreaves, R. J. The Role of Molecular Imaging in Drug Discovery and Development. *Clin. Pharmacol. Ther.* **2008**, *83*, 349–353.
(29) Acton, P. D.; Kung, M.-P.; Mu, M.; Plössl, K.; Hou, C.; Siciliano, M.; Oya, S.; Kung, H. F. Single-Photon Emission Tomography Imaging of Serotonin Transporters in the Non-Human Primate Brain with the Selective Radioligand [^{123}I]IDAM. *Eur. J. Nucl. Med.* **1999**, *26*, 854–861.
(30) Wilson, A. A.; Ginovart, N.; Schmidt, M.; Meyer, J. H.; Threlkeld, P. G.; Houle, S. Novel Radiotracers for Imaging the Serotonin Transporter by Positron Emission Tomography: Synthesis, Radiosynthesis, and in Vitro and ex Vivo Evaluation of ^{11}C-Labeled 2-(Phenylthio)araalkylamines. *J. Med. Chem.* **2000**, *43*, 3103–3110.
(31) Ginovart, N.; Wilson, A. A.; Meyer, J. H.; Hussey, D.; Houle, S. Positron Emission Tomography Quantification of [^{11}C]-DASB Binding

to the Human Serotonin Transporter: Modeling Strategies. *J. Cereb. Blood Flow Metab.* **2001**, *21*, 1342–1353.
(32) Emond, P.; Vercouillie, J.; Innis, R.; Chalon, S.; Mavel, S.; Frangin, Y.; Halldin, C.; Besnard, J.-C.; Guilloteau, D. Substituted Diphenyl Sulfides as Selective Serotonin Transporter Ligands: Synthesis and In Vitro Evaluation. *J. Med. Chem.* **2002**, *45*, 1253–1258.
(33) Huang, Y.; Hwang, D.-R.; Narendran, R.; Sudo, Y.; Chatterjeee, R.; Bae, S.-A.; Mawlawi, O.; Kegeles, L. S.; Wilson, A. A.; Kung, H. F.; Laruelle, M. Comparative Evaluation in Nonhuman Primates of Five PET Radiotracers for Imaging the Serotonin Transporters: [^{11}C]MCN5652, [^{11}C]ADAM, [^{11}C]DASB, [^{11}C]DAPA, and [^{11}C]AFM. *J. Cereb. Blood Flow Metab.* **2002**, *22*, 1377–1398.
(34) Szabo, Z.; McCann, U. D.; Wilson, A. A.; Scheffel, U.; Owonikoko, T.; Mathews, W. B.; Ravert, H. T.; Hilton, J.; Dannals, R. F.; Ricaurte, G. A. Comparison of (+)-11C-McN5652 and 11C-DASB as Serotonin Transporter Radioligands Under Various Experimental Conditions. *J. Nucl. Med.* **2002**, *43*, 678–692.
(35) Wellsow, J.; Kovar, K.-A.; Machulla, H.-J. Molecular Modeling of Potential New and Selective PET Radiotracers for the Serotonin Transporter. *J. Pharm. Pharmaceut. Sci.* **2002**, *5*, 245–257.
(36) Huang, Y.; Bae, S.; Zhu, Z.; Guo, N.; Roth, B. L.; Laruelle, M. Fluorinated Diaryl Sulfides as Serotonin Transporter Ligands: Synthesis, Structure-Activity Relationship Study, and in Vivo Evaluation of Fluorine-18-Labeled Compounds as PET Imaging Agents. *J. Med. Chem.* **2005**, *48*, 2559–2570.
(37) Jarkas, N.; Votaw, J. R.; Voll, R. J.; Williams, L.; Camp, V. M.; Owens, M. J.; Purselle, D. C.; Bremner, J. D.; Kilts, C. D.; Nemeroff, C. B.; Goodman, M. M. Carbon-11 HOMADAM: A Novel PET Radiotracer for Imaging Serotonin Transporters. *Nucl. Med. Biol.* **2005**, *32*, 211–224.
(38) Fang, P.; Shiue, G. G.; Shimazu, T.; Greenberg, J. H.; Shiue, C.-Y. Synthesis and Evaluation of *N,N*-Dimethyl-2-(2-amino-5-[^{18}F]fluorophenylthio)benzylamine (5-[^{18}F]-ADAM) as a Serotonin Transporter Imaging Agent. *Appl. Radiat. Isot.* **2004**, *61*, 1247–1254.
(39) Garg, S.; Thopate, S. R.; Minton, R. C.; Black, K. W.; Lynch, A. J. H.; Garg, P. K. 3-Amino-4-(2-((4-[^{18}F]fluorobenzyl)methylamino)methylphenylsulfanyl)benzonitrile, an F-18 Fluorobenzyl Analogue of DASB: Synthesis, in Vitro Binding, and in Vivo Biodistribution Studies. *Bioconj. Chem.* **2007**, *18*, 1612–1618.
(40) Parhi, A. K.; Wang, J. L.; Oya, S.; Choi, S.-R.; Kung, M.-P.; Kung, H. F. 2-(2′-((Dimethylamino)methyl)-4′-(fluoroalkoxy)-phenylthio)benzenamine Derivatives as Serotonin Transporter Imaging Agents. *J. Med. Chem.* **2007**, *50*, 6673–6684.
(41) Jarkas, N.; Voll, R. J.; Williams, L.; Votaw, J. R.; Owens, M.; Goodman, M. M. Synthesis and In Vivo Evaluation of Halogenated *N,N*-Dimethyl-2-(2′-amino-4′-hydroxymethylphenylthio)benzylamine Derivatives as PET Serotonin Transporter Ligands. *J. Med. Chem.* **2008**, *51*, 271–281.
(42) Mavel, S.; Vercouillie, J.; Garreau, L.; Raguza, T.; Ravna, A. W.; Chalon, S.; Guilloteau, D.; Emond, P. Docking Study, Synthesis, and In Vitro Evaluation of Fluoro-MADAM Derivatives as SERT Ligands for PET Imaging. *Bioorg. Med. Chem.* **2008**, *16*, 9050–9055.
(43) Wang, J. L.; Parhi, A. K.; Oya, S.; Lieberman, B.; Kung, M.-P.; Kung, H. F. 2-(2′-((Dimethylamino)methyl)-4′-(3-[^{18}F]fluoropropoxy)-phenylthio)benzenamine for Positron Emission Tomography Imaging of Serotonin Transporters. *Nucl. Med. Biol.* **2008**, *35*, 447–458.
(44) Bois, F.; Baldwin, R. M.; Kula, N. S.; Baldessarini, R. J.; Innis, R. B.; Tamagnan, G. Synthesis and Monoamine Transporter Affinity of 3′-Analogs of 2-β-Carbomethoxy-3-β-(4′-iodophenyl)tropane (β-CIT). *Bioorg. Med. Chem. Lett.* **2004**, *14*, 2117–2120.
(45) Peng, X.; Zhang, A.; Kula, N. S.; Baldessarini, R. J.; Neumeyer, J. L. Synthesis and Amine Transporter Affinities of Novel Phenyltropane Derivatives as Potential Positron Emission Tomography (PET) Imaging Agents. *Bioorg. Med. Chem. Lett.* **2004**, *14*, 5635–5639.
(46) Tamagnan, G.; Alagille, D.; Fu, X.; Kula, N. S.; Baldessarini, R. J.; Innis, R. B.; Baldwin, R. M. Synthesis and Monoamine Transporter Affinity of New 2β-Carbomethoxy-3β-[4-(Substituted Thiophenyl)]Phenyltropanes: Discovery of a Selective SERT Antagonist with Picomolar Potency. *Bioorg. Med. Chem. Lett.* **2005**, *15*, 1131–1133.
(47) Levin, C. S.; Hoffman, E. J. Calculation of Positron Range and Its Effect on the Fundamental Limit of Positron Emission Tomography System Spatial Resolution. *Phys. Med. Biol.* **1999**, *44*, 781–799.
(48) Wernick, M. N.; Aarsvold, J. N. *Emission Tomography: The Fundamentals of PET and SPECT*. Elsevier Academic Press: San Diego, CA, 2004.
(49) Böhm, H.-J.; Banner, D.; Bendels, S.; Kansy, M.; Kuhn, B.; Müller, K.; Obst-Sander, U.; Stahl, M. Fluorine in Medicinal Chemistry. *ChemBioChem* **2004**, *5*, 637–643.
(50) Müller, K.; Faeh, C.; Diederich, F. Fluorine in Pharmaceuticals: Looking Beyond Intuition. *Science* **2007**, *317*, 1881–1886.
(51) Hagmann, W. K. The Many Roles for Fluorine in Medicinal Chemistry. *J. Med. Chem.* **2008**, *51*, 4359–4369.
(52) Lasne, M.-C.; Perrio, C.; Rouden, J.; Barré, 940 > e, L.; Roeda, D.; Dollé, 940 > e, F.; Crouzel, C. Chemistry of β^+-Emitting Compounds Based on Fluorine-18. *Top. Curr. Chem.* **2002**, *222*, 201–258.
(53) Cai, L.; Lu, S.; Pike, V. W. Chemistry with [^{18}F]Fluoride Ion. *Eur. J. Org. Chem.* **2008**, 2853–2873.
(54) Kirk, K. L. Fluorination in Medicinal Chemistry: Methods, Strategies, and Recent Developments. *Org. Proc. Res. Dev.* **2008**, *12*, 305–321.
(55) Elfving, B.; Madsen, J.; Knudsen, G. M. Neuroimaging of the Serotonin Reuptake Site Requires High-Affinity Ligands. *Synapse* **2007**, *61*, 882–888.
(56) Dischino, D. D.; Welch, M. J.; Kilbourn, M. R.; Raichle, M. E. Relationship Between Lipophilicity and Brain Extraction of C-11-Labeled Radiopharmaceuticals. *J. Nucl. Med.* **1983**, *24*, 1030–1038.
(57) Elfving, B.; Bjørnholm, B.; Ebert, B.; Knudsen, G. M. Binding Characteristics of Selective Serotonin Reuptake Inhibitors With Relation to Emission Tomography Studies. *Synapse* **2001**, *41*, 203–211.
(58) Waterhouse, R. N. Determination of Lipophilicity and Its Use as a Predictor of Blood-Brain Barrier Penetration of Molecular Imaging Agents. *Mol. Imag. Biol.* **2003**, *5*, 376–389.
(59) Kish, S. J.; Furukawa, Y.; Chang, L.-J.; Tong, J.; Ginovart, N.; Wilson, A.; Houle, S.; Meyer, J. H. Regional Distribution of Serotonin Transporter Protein in Postmortem Human Brain. Is the Cerebellum a SERT-Free Brain Region? *Nuc. Med. Biol.* **2005**, *32*, 123–128.
(60) Goodman, M. M.; Chen, P.; Plisson, C.; Martarello, L.; Galt, J.; Votaw, J. R.; Kilts, C. D.; Malveaux, G.; Camp, V. M.; Shi, B.; Ely, T. D.; Howell, L.; McConathy, J.; Nemeroff, C. B. Synthesis and Characterization of Iodine-123 Labeled 2β-Carbomethoxy-3β-(4′-((Z)-2-iodoethenyl)phenyl)nortropane. A Ligand for in vivo Imaging of Serotonin Transporters by Single-Photon-Emission Tomography. *J. Med. Chem.* **2003**, *46*, 925–935.
(61) Plisson, C.; McConathy, J.; Martarello, L.; Malveaux, E. J.; Camp, V. M.; Williams, L.; Votaw, J. R.; Goodman, M. M. Synthesis, Radiosynthesis, and Biological Evaluation of Carbon-11 and Iodine-123 Labeled 2β-Carbomethoxy-3β-[4′-((Z)-2-haloethenyl)phenyl]tropanes: Candidate Radioligands for in Vivo Imaging of the Serotonin Transporter. *J. Med. Chem.* **2004**, *47*, 1122–1135.
(62) Plisson, C.; Jarkas, N.; McConathy, J.; Voll, R. J.; Votaw, J.; Williams, L.; Howell, L. L.; Kilts, C. D.; Goodman, M. M. Evaluation of Carbon-11-Labeled 2β-Carbomethoxy-3β-[4′-((Z)-2-iodoethenyl)phenyl]nortropane as a Potential Radioligand for Imaging the Serotonin Transporter by PET. *J. Med. Chem.* **2006**, *49*, 942–946.
(63) Stehouwer, J. S.; Jarkas, N.; Zeng, F.; Voll, R. J.; Williams, L.; Owens, M. J.; Votaw, J. R.; Goodman, M. M. Synthesis, Radiosynthesis, and Biological Evaluation of Carbon-11 Labeled 2β-Carbomethoxy-3β-(3′-((Z)-2-haloethenyl)phenyl)nortropanes: Candidate Radioligands for In Vivo Imaging of the Serotonin Transporter with Positron Emission Tomography. *J. Med. Chem.* **2006**, *49*, 6760–6767.
(64) Plisson, C.; Stehouwer, J. S.; Voll, R. J.; Howell, L. L.; Votaw, J. R.; Owens, M. J.; Goodman, M. M. Synthesis and In Vivo Evaluation of Fluorine-18 and Iodine-123 Labeled 2β-Carbo(2-fluoroethoxy)-3β-(4′-((*Z*)-2-iodoethenyl)phenyl)nortropane as a Candidate Serotonin Transporter Imaging Agent. *J. Med. Chem.* **2007**, *50*, 4553–4560.
(65) Seibyl, J.; Goodman, M.; Koren, A.; Stehouwer, J.; Jennings, D.; Staley, J.; Tamagnan, G. Preclinical and Clinical Characterization of 123-I *m*ZIENT, a Marker of Serotonin Transporter Density. *J. Nucl. Med.* **2007**, *48*, 113P.
(66) Tamagnan, G.; Stehouwer, J.; Staley, J. K.; Megyola, C.; Koren, A.; Goodman, M.; Seibyl, J. In Vivo Characterization in Subhuman Primates of *m*ZIENT: A New Serotonin Transporter, Effects of Selective SERT Displacement. *NeuroImage* **2006**, *31*, T131.
(67) Stehouwer, J. S.; Plisson, C.; Jarkas, N.; Zeng, F.; Voll, R. J.; Williams, L.; Martarello, L.; Votaw, J. R.; Tamagnan, G.; Goodman, M. M. Synthesis, Radiosynthesis, and Biological Evaluation of Carbon-11 and Fluorine-18 (*N*-Fluoroalkyl) Labeled 2β-Carbomethoxy-3β-(4′-(3-furyl)phenyl)-tropanes and -nortropanes: Candidate Radioligands for in Vivo Imaging of the Serotonin Transporter with Positron Emission Tomography. *J. Med. Chem.* **2005**, *48*, 7080–7083.
(68) Stehouwer, J.; Jarkas, N.; Zeng, F.; Voll, R.; Williams, L.; Votaw, J.; Goodman, M. MicroPET Imaging of the Brain Serotonin Transporter with [^{18}F]βFE*m*ZIENT. *J. Nucl. Med.* **2006**, *47*, 27P.
(69) Goodman, M.; Stehouwer, J.; Jarkas, N.; Voll, R.; Williams, L.; Votaw, J. In Vivo Characterization in Non-Human Primates of βFEmZIENT and βFEmZBrENT: New Serotonin Transporter Imaging Agents: Effects of Selective Monoamine Transporter Displacement Using MicroPET. *Neuroimage* **2006**, *31*, T27.
(70) Stehouwer, J.; Jarkas, N.; Zeng, F.; Voll, R.; Williams, L.; Votaw, J.; Goodman, M. MicroPET Imaging of the CNS Serotonin Transporter with [^{18}F]FP*m*ZIENT and [^{18}F]FP*m*ZBrENT. Presented at The Southeastern Regional Meeting of the American Chemical Society, November 1−4, 2006, Augusta, GA; Abstract #525.
(71) Carroll, F. I.; Kotian, P.; Dehghani, A.; Gray, J. L.; Kuzemko, M. A.; Parham, K. A.; Abraham, P.; Lewin, A. H.; Boja, J. W.; Kuhar, M. J.

Cocaine and 3β-(4′-Substituted phenyl)tropane-2β-carboxylic Acid Ester and Amide Analogues. New High-Affinity and Selective Compounds for the Dopamine Transporter. *J. Med. Chem.* **1995**, *38*, 379–388.

(72) Blough, B. E.; Abraham, P.; Lewin, A. H.; Kuhar, M. J.; Boja, J. W.; Carroll, F. I. Synthesis and Transporter Binding Properties of 3β-(4′-Alkyl-, 4′-alkenyl-, and 4′-alkynylphenyl)nortropane-2β-carboxylic Acid Methyl Esters: Serotonin Transporter Selective Analogs. *J. Med. Chem.* **1996**, *39*, 4027–4035.

(73) Mitchell, T. N.; Amamria, A.; Killing, H.; Rutschow, D. Palladium Catalysis in Organotin Chemistry: Addition of Hexaalkylditins to Alkynes. *J. Organomet. Chem.* **1986**, *304*, 257–265.

(74) Blough, B. E.; Keverline, K. I.; Nie, Z.; Navarro, H.; Kuhar, M. J.; Carroll, F. I. Synthesis and Transporter Binding Properties of 3β-[4′-(Phenylalkyl, -phenylalkenyl, and -phenyalkynl)phenyl]tropane-2β-carboxylic Acid Methyl Esters: Evidence of a Remote Phenyl Binding Domain on the Dopamine Transporter. *J. Med. Chem.* **2002**, *45*, 4029–4037.

(75) Lemaire, C.; Plenevaux, A.; Aerts, J.; Del Fiore, G.; Brihaye, C.; Le Bars, D.; Comar, D.; Luxen, A. Solid Phase Extraction - An Alternative to the Use of Rotary Evaporators for Solvent Removal in the Rapid Formulation of PET Radiopharmaceuticals. *J. Labelled Compd. Radiopharm.* **1999**, *42*, 63–75.

(76) Wilson, A. A.; Houle, S. Radiosynthesis of Carbon-11 Labelled N-Methyl-2-(arylthio)benzylamines: Potential Radiotracers for the Serotonin Reuptake Receptor. *J. Labelled Compd. Radiopharm.* **1999**, *42*, 1277–1288.

(77) Wilson, A. A.; Jin, L.; Garcia, A.; DaSilva, J. N.; Houle, S. An Admonition When Measuring the Lipophilicity of Radiotracers Using Counting Techniques. *Appl. Radiat. Isot.* **2001**, *54*, 203–208.

(78) Owens, M. J.; Morgan, W. N.; Plott, S. J.; Nemeroff, C. B. Neurotransmitter Receptor and Transporter Binding Profile of Antidepressants and Their Metabolites. *J. Pharmacol. Exp. Ther.* **1997**, *283*, 1305–1322.

(79) Hiemke, C.; Härtter, S. Pharmacokinetics of Selective Serotonin Reuptake Inhibitors. *Pharmacol. Therap.* **2000**, *85*, 11–28.

(80) Boja, J. W.; Patel, A.; Carroll, F. I.; Rahman, M. A.; Philip, A.; Lewin, A. H.; Kopajtic, T. A.; Kuhar, M. J. [^{125}I]RTI-55: a potent ligand for dopamine transporters. *Eur. J. Pharmacol.* **1991**, *194*, 133–134.

(81) Cheetham, S. C.; Viggers, J. A.; Butler, S. A.; Prow, M. R.; Heal, D. J. [^{3}H]Nisoxetine - A Radioligand for Noradrenaline Reuptake Sites: Correlation With Inhibition of [^{3}H]Noradrenaline Uptake and Effects of DSP-4 Lesioning and Antidepressant Treatments. *Neuropharmacology* **1996**, *35*, 63–70.

(82) Hrdina, P. D.; Foy, B.; Hepner, A.; Summers, R. J. Antidepressant Binding Sites in Brain: Autoradiographic Comparison of [^{3}H]Paroxetine and [^{3}H]Imipramine Localization and Relationship to Serotonin Transporter. *J. Pharmacol. Exp. Ther.* **1990**, *252*, 410–418.

(83) Cortés, R.; Soriano, E.; Pazos, A.; Probst, A.; Palacios, J. M. Autoradiography of Antidepressant Binding Sites in the Human Brain: Localization Using [^{3}H]Imipramine and [^{3}H]Paroxetine. *Neuroscience* **1988**, *27*, 473–496.

(84) Potter, P. M.; Wadkins, R. M. Carboxylesterases—Detoxifying Enzymes and Targets for Drug Therapy. *Curr. Med. Chem.* **2006**, *13*, 1045–1054.

(85) Elfving, B.; Bjørnholm, B.; Knudsen, G. M. Interference of Anaesthetics With Radioligand Binding in Neuroreceptor Studies. *Eur. J. Nucl. Med. Mol. Imaging* **2003**, *30*, 912–915.

(86) Votaw, J.; Byas-Smith, M.; Hua, J.; Voll, R.; Martarello, L.; Levey, A. I.; Bowman, F. D.; Goodman, M. Interaction of Isoflurane With the Dopamine Transporter. *Anesthesiology* **2003**, *98*, 404–411.

(87) McCormick, P. N.; Ginovart, N.; Vasdev, N.; Seeman, P.; Kapur, S.; Wilson, A. A. Isoflurane Increases Both the Specific Binding Ratio and Sensitivity to Amphetamine Challenge of [^{11}C]-(+)-PHNO. *Neuroimage* **2006**, *31*, T33.

(88) Tsukada, H.; Nishiyama, S.; Kakiuchi, T.; Ohba, H.; Sato, K.; Harada, N. Ketamine Alters the Availability of Striatal Dopamine Transporter as Measured by [^{11}C]β-CFT and [^{11}C]β-CIT-FE in the Monkey Brain. *Synapse* **2001**, *42*, 273–280.

(89) Katz, J. L.; Izenwasser, S.; Terry, P. Relationships Among Dopamine Transporter Affinities and Cocaine-Like Discriminative-Stimulus Effects. *Psychopharmacology* **2000**, *148*, 90–98.

(90) Cook, C. D.; Carroll, F. I.; Beardsley, P. M. RTI 113, a 3-Phenyltropane Analog, Produces Long-Lasting Cocaine-Like Discriminative Stimulus Effects in Rats and Squirrel Monkeys. *Eur. J. Pharmacol.* **2002**, *442*, 93–98.

(91) Wilcox, K. M.; Lindsey, K. P.; Votaw, J. R.; Goodman, M. M.; Martarello, L.; Carroll, F. I.; Howell, L. L. Self-Administration of Cocaine and the Cocaine Analog RTI-113: Relationship to Dopamine Transporter Occupancy Determined by PET Neuroimaging in Rhesus Monkeys. *Synapse* **2002**, *43*, 78–85.

(92) Wong, E. H. F.; Sonders, M. S.; Amara, S. G.; Tinholt, P. M.; Piercey, M. F. P.; Hoffmann, W. P.; Hyslop, D. K.; Franklin, S.; Porsolt, R. D.; Bonsignori, A.; Carfagna, N.; McArthur, R. A. Reboxetine: A Pharmacologically Potent, Selective, and Specific Norepinephrine Reuptake Inhibitor. *Biol. Psychiatry* **2000**, *47*, 818–829.

(93) Patient Selection and Antidepressant Therapy With Reboxetine, A New Selective Norepinephrine Reuptake Inhibitor. *J. Clin. Psychiatry*, **1998**, *59*, Supplement 14.

JM800781A